NACA TN 4181

10520

NATIONAL ADVISORY COMMITTEE
FOR AERONAUTICS

TECHNICAL NOTE 4181

INVESTIGATION OF THE EFFECTS OF PROPELLER DIAMETER ON THE

ABILITY OF A FLAPPED WING, WITH AND WITHOUT

BOUNDARY-LAYER CONTROL, TO DEFLECT A

PROPELLER SLIPSTREAM DOWNWARD

FOR VERTICAL TAKE-OFF

By Kenneth P. Spreemann

Langley Aeronautical Laboratory
Langley Field, Va.

Washington
December 1957

NATIONAL ADVISORY COMMITTEE FOR AERONAUTICS

TECHNICAL NOTE 4181

INVESTIGATION OF THE EFFECTS OF PROPELLER DIAMETER ON THE

ABILITY OF A FLAPPED WING, WITH AND WITHOUT

BOUNDARY-LAYER CONTROL, TO DEFLECT A

PROPELLER SLIPSTREAM DOWNWARD

FOR VERTICAL TAKE-OFF

By Kenneth P. Spreemann

SUMMARY

An investigation has been made to study the effects of propeller diameter on the ability of a flapped wing, with and without boundary-layer control, to deflect propeller slipstreams downward for vertical take-off.

The results of the investigation indicate that without boundary-layer control an increase in the ratio of flap chord to propeller diameter increases the turning angle but decreases the ratio of resultant force to thrust, either in or out of the region of ground effects. It appears that the ratios of flap chord to propeller diameter used in the investigation (0.25 to 0.375) were too low to provide the turning angles normally required for vertical take-off without boundary-layer control. The results also indicate that the increment of turning angle and the increment of the ratio of resultant force to thrust due to boundary-layer control are, in general, independent of the ratio of flap chord to propeller diameter.

INTRODUCTION

The Langley 7- by 10-Foot Tunnels Branch is conducting an investigation of various wing-flap configurations in an effort to develop relatively simple arrangements capable of deflecting the propeller slipstream downward for vertical take-off. The capabilities of some of these configurations are reported in references 1 to 6. In these references, investigations have been reported that cover many variables that can affect the turning angle, pitching moments, and performance, such

as employing leading-edge slats, hinging the flap farther forward on the wing to reduce the diving moments, and boundary-layer control by blowing over the flap for improving the turning angles and resultant force. It has been shown in reference 7 that the ratio of flap chord to propeller diameter is one of the primary geometric variables governing the amount of slipstream deflection that can be obtained without boundary-layer control. Also, the investigation reported in reference 6 indicates that boundary-layer control by blowing can aid the turning of the slipstream; however, the model employed in that investigation had a rather large ratio of flap chord to propeller diameter, and thus provided reasonably large turning angles without boundary-layer control.

The present investigation was undertaken to explore the possibility that the turning angles obtained with a smaller ratio of flap chord to propeller diameter might be greatly increased through the use of boundary-layer control. The investigation was conducted in a static-thrust facility at the Langley Aeronautical Laboratory and employed a model equipped with plain flaps of 50.4-percent chord and 25-percent chord.

SYMBOLS

The positive sense of forces, moments, and angles used in this paper is indicated in figure 1. Moments are referred to the 0.25 point of the mean aerodynamic chord.

$b/2$ span of semispan wing, 2.0 ft

D propeller diameter, ft

h height of wing trailing edge above ground, ft

$\delta_{f,1}$ deflection of forward flap, deg

$\delta_{f,2}$ deflection of rear flap, deg

x longitudinal distance from propeller to wing leading edge, ft

L lift, lb

F_X longitudinal force (Thrust - Drag), lb

M pitching moment, ft-lb

F resultant force, lb

T propeller thrust, 15 lb

θ turning angle (inclination of resultant-force vector from thrust axis), $\tan^{-1}\dfrac{L}{F_X}$, deg

C_μ'' momentum coefficient, $\dfrac{Q_n \rho_n V_n}{q''S}$

C_q'' flow coefficient, $\dfrac{Q_n}{V''S}$

C_p'' pressure coefficient, $\dfrac{p - p''}{q''}$

P power in blowing system, $\dfrac{\rho_n \frac{Z}{12} \frac{b}{2} V_n^3}{2}$, ft-lb/sec

P'' power in slipstream, $\dfrac{\rho'' \frac{\pi}{4} D^2 (V'')^3}{4}$, ft-lb/sec

Q_n rate of air flow out of nozzle expanded to slipstream static pressure, cu ft/sec

ρ_n mass density of air blown out of nozzle, slugs/cu ft

V_n nozzle exit velocity (assuming isentropic expansion to slipstream static pressure), ft/sec

ρ'' mass density of air in slipstream, slugs/cu ft

V'' average slipstream velocity, ft/sec

q'' average slipstream dynamic pressure, $\dfrac{T}{\pi D^2/4}$, lb/sq ft

S wing area of semispan model, 2.0 sq ft

p static pressure in blowing system, lb/sq ft

p'' slipstream static pressure, lb/sq ft

Z effective nozzle gap, in.

c wing chord, 1.0 ft

c_f flap chord, ft

c_b propeller blade-element chord, ft

t propeller blade-element thickness, ft

R propeller tip radius, ft

r radius to propeller blade element, ft

β propeller blade-element angle, deg

η propeller efficiency, $\dfrac{TV''}{2\pi nQ}$

n propeller rotational speed, rps

Q propeller torque, lb-ft

APPARATUS AND METHOD

Since the present investigation was considered to be primarily of
a qualitative nature, it was considered expedient to use only one wing-
flap model and obtain the desired ratios of flap chord to propeller
diameter by varying the propeller diameter. A drawing of the model with
pertinent dimensions is presented in figure 2, and a photograph of the
model mounted for testing is shown in figure 3. The geometric character-
istics of the model wing are given in the following table:

Area (semispan), sq ft 2.0
Span (semispan), ft 2.0
Chord, ft 1.0
Airfoil section . . . . NACA 4415

The propeller diameters used were 2, 1.67, and 1.33 feet. The two
smaller propellers were made by successively cutting off the tips of the
larger propeller. For the blade angles employed on these propellers the
static efficiency varied from 60 to 66 percent. The physical character-
istics of the three propellers are presented in figures 4, 5, and 6.

The forward flap was hinged at the 0.504 wing-chord station (fig. 2). The rear flap was made by sawing off the trailing 25 percent of the wing and reattaching it with a piano hinge. With the flap deflected, the gap at the hinge line was filled and faired with modeling clay.

For these tests, the propeller was mounted independently as shown in figures 2 and 3. The thrust axis was always parallel to the wing-chord plane. The propeller was driven by an electric motor which was mounted inside a nacelle by means of strain-gage beams in such a way that the propeller thrust and torque could be measured. The lift, longitudinal force, and pitching moment of the wing model were measured on a strain-gage balance at the root of the wing. In reducing the data from these tests, the propeller thrust was included.

The full-span blowing nozzle (approximate chordwise shape shown in fig. 2) had an effective gap of about 0.017 inch for all tests. The ratio of power in the blowing system to power in the slipstream, the pressure coefficient, and the flow coefficient are plotted against momentum coefficient in figure 7. The mass flow through the nozzle was measured by means of a standard sharp-edge-orifice flowmeter. Air was supplied at a pressure of 90 pounds per square inch through a 1/2-inch line.

The ground was simulated by a sheet of plywood as shown in figures 1 and 3. All tests in the presence of the ground were conducted with an angle of 20° between the ground board and the thrust axis of the propeller. The ground board extended about 2 feet beyond the propeller plane and about 4 feet behind the trailing edge of the wing.

The investigation was conducted in a static-thrust facility at the Langley Aeronautical Laboratory. All data were obtained at zero forward velocity with a static thrust of 15 pounds from the propeller. Therefore, the velocity in the slipstream varied inversely with propeller diameter, and the Reynolds numbers based on the chord of the wing were 0.39×10^6, 0.47×10^6, and 0.59×10^6 for the 2-foot-, 1.67-foot-, and 1.33-foot-diameter propellers, respectively. Inasmuch as the tests were conducted under static conditions in a large room, none of the corrections that are normally applicable to wind-tunnel tests were employed.

RESULTS AND DISCUSSION

The data are presented in the figures as follows:

It should be remembered that a single propeller was used in this investigation. Previous work has indicated that better thrust recovery is usually obtained when two propellers are employed. (For example, see ref. 1.)

It has been shown in reference 7 that the ratio of flap chord to propeller diameter is an important parameter in governing the amount of slipstream deflection that can be obtained without boundary-layer control. The present investigation was undertaken to study the effect of varying propeller diameter on a wing and flap of fixed chord, with and without boundary-layer control.

Effects of c_f/D Out of Region of Ground Effects

Out of the region of ground effects and without boundary-layer control, c_f/D usually had little effect on θ and F/T when the forward flap was deflected at a small angle (fig. 8). For larger deflections, θ generally increased and F/T generally decreased with increases in c_f/D (figs. 9 to 11). Deflection of both flaps (figs. 12 to 15) produced results similar to those for single-flap deflection.

Boundary-layer control increased both the turning and the ratio of resultant force to thrust. As was shown in reference 6, boundary-layer control is most effective at the highest flap deflections where the air flow over the flap is separated without boundary-layer control. At low momentum coefficients the increments of θ and F/T due to boundary-layer control were largest for the larger ratios of flap chord to propeller diameter. At high momentum coefficients the increments of θ and F/T due to blowing over the flap were, in general, the same for all ratios of flap chord to propeller diameter within the limits of this investigation.

The nondimensional diving moments $\frac{M}{TD}$ were in some cases more than doubled with an increase of c_f/D from 0.25 to 0.375. (See figs. 8 to 15.) These large increases are apparent because the moments are non-dimensionalized on the basis of the individual propeller diameters. However, when the moments are nondimensionalized on the basis of the chord of the wing, the data still indicate increases of 40 to 50 per-cent. (See fig. 16.) It should be noted that, if the ratio of flap chord to propeller diameter had been achieved by holding the propeller diameter and wing chord constant while increasing the flap chord (that is, by moving the flap hinge line closer to the moment reference point), the diving moments would be reduced with increases in c_f/D.

An idea of the power required in the blowing system can be obtained from part (e) of figures 9 to 15. The ratio P/P'' represents the ratio of power in the blowing system to power in the slipstream. It can be seen that most of the gains in turning angle were made at relatively low power ratios.

Effects of c_f/D in Proximity to Ground

In the region of ground effects, both the angle through which the slipstream is deflected and the ratio of resultant force to thrust showed trends similar to those in previous investigations (for example, refs. 5 and 6) regardless of the ratio of flap chord to propeller diam-eter. A comparison of the (b) parts of figure 10 and figures 17 to 19 illustrate these trends, which are characteristically a reduction of F/T as the ground is approached, followed by sizable recoveries very near the ground, with or without boundary-layer control.

Effects of c_f/D at Selected Momentum Coefficient

It is shown in figures 20 to 23 that, with $\delta_{f,1} = 70^{\circ}$ and $\delta_{f,2} = 0^{\circ}$, the turning angle always increased with increases in c_f/D, whereas F/T usually decreased with increases in c_f/D except at $C_{\mu}'' = 0.09$, where F/T remained fairly constant, regardless of height above the ground. With a double-flap deflection of $\delta_{f,1} = 60^{\circ}$ and $\delta_{f,2} = 30^{\circ}$ (fig. 24), θ displayed about the same characteristics out of the region of ground effects as were obtained with the single-flap configuration. On the other hand, F/T was always reduced with increased c_f/D for the double-flap configurations.

Summary Data

The optimum values of the ratio of resultant force to thrust, turning angle, and pitching moment obtained from the best flap deflections for the different ratios of flap chord to propeller diameter are presented in figure 25. There is an overall increase in θ and F/T with increase in c_f/D, and the diving moments are consistently increased with increases in c_f/D and turning angle. As previously mentioned, the indicated changes in the diving moments attributable to c_f/D would be about halved if the moments were referred to the mean aerodynamic chord of the wing rather than the propeller diameter. From figure 25 it appears that increases in C_μ'' have a greater effect on the turning angle and F/T than increases in c_f/D for the range of c_f/D investigated.

The average variation of turning angle with ratio of flap chord to propeller diameter is presented in figure 26. Included in this figure for comparison with the present investigation are results from references 1 and 2 as summarized in reference 7. The data of this investigation follow the trends of the data from references 1 and 2, although the actual values of this investigation indicate lower turning angles at the higher values of c_f/D than those of the reference data. This difference might be due to the selection of better wing-flap configurations in the reference investigations.

CONCLUDING REMARKS

Without boundary-layer control, increases in the ratio of flap chord to propeller diameter increased the turning angle but decreased the ratio of resultant force to thrust, either in or out of the region of ground effects. It appears that the values of the ratios of flap chord to propeller diameter (0.25 to 0.375) were too low to provide the turning angles normally required for vertical take-off without boundary-layer control. Also, the ratio of resultant force to thrust was low, probably because only one propeller was employed.

The results of the investigation indicate that the increment of turning angle and the increment of the ratio of resultant force to

thrust due to boundary-layer control were, in general, independent of the ratio of flap chord to propeller diameter.

Langley Aeronautical Laboratory,
      National Advisory Committee for Aeronautics,
            Langley Field, Va., September 23, 1957.

REFERENCES

1. Kuhn, Richard E., and Draper, John W.: An Investigation of a Wing-
      Propeller Configuration Employing Large-Chord Plain Flaps and
      Large-Diameter Propellers for Low-Speed Flight and Vertical Take-
      Off. NACA TN 3307, 1954.

2. Kuhn, Richard E., and Draper, John W.: Investigation of Effective-
      ness of Large-Chord Slotted Flaps in Deflecting Propeller Slip-
      streams Downward for Vertical Take-Off and Low-Speed Flight. NACA
      TN 3364, 1955.

3. Kuhn, Richard E.: Investigation at Zero Forward Speed of a Leading-
      Edge Slat as a Longitudinal Control Device for Vertically Rising
      Airplanes That Utilize the Redirected-Slipstream Principle.
      NACA TN 3692, 1956.

4. Kuhn, Richard E., and Spreemann, Kenneth P.: Preliminary Investiga-
      tion of the Effectiveness of a Sliding Flap in Deflecting a
      Propeller Slipstream Downward for Vertical Take-Off. NACA TN 3693,
      1956.

5. Kuhn, Richard E.: Investigation of the Effects of Ground Proximity
      and Propeller Position on the Effectiveness of a Wing with Large-
      Chord Slotted Flaps in Redirecting Propeller Slipstreams Downward
      for Vertical Take-Off. NACA TN 3629, 1956.

6. Spreemann, Kenneth P., and Kuhn, Richard E.: Investigation of the
      Effectiveness of Boundary-Layer Control by Blowing Over a Combina-
      tion of Sliding and Plain Flaps in Deflecting a Propeller Slip-
      stream Downward for Vertical Take-Off. NACA TN 3904, 1956.

7. McKinney, M. O., Kuhn, R. E., and Hammack, J. B.: Problems in the
      Design of Propeller-Driven Vertical Take-Off Transport Airplanes.
      Aero. Eng. Rev., vol. 15, no. 4, Apr. 1956, pp. 68-75, 84.
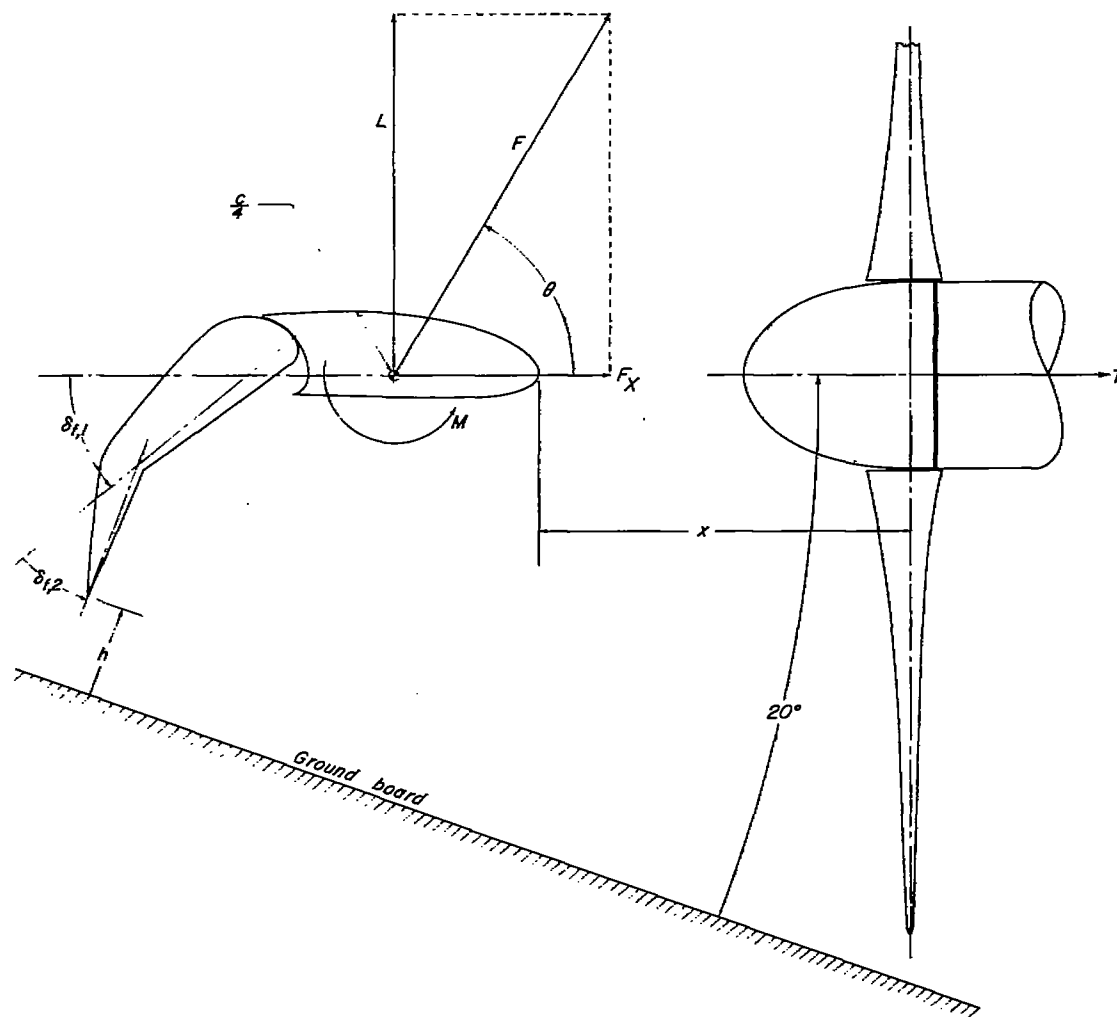
Figure 1.- Positive sense of forces, moments, and angles.

Full-span
nozzle at .48c

Plenum chamber

.104c

.03lc

.504c

c = 1200

25c

10.0

Balance center at .25c

24

12¼

12

10

8

⅛

Balance
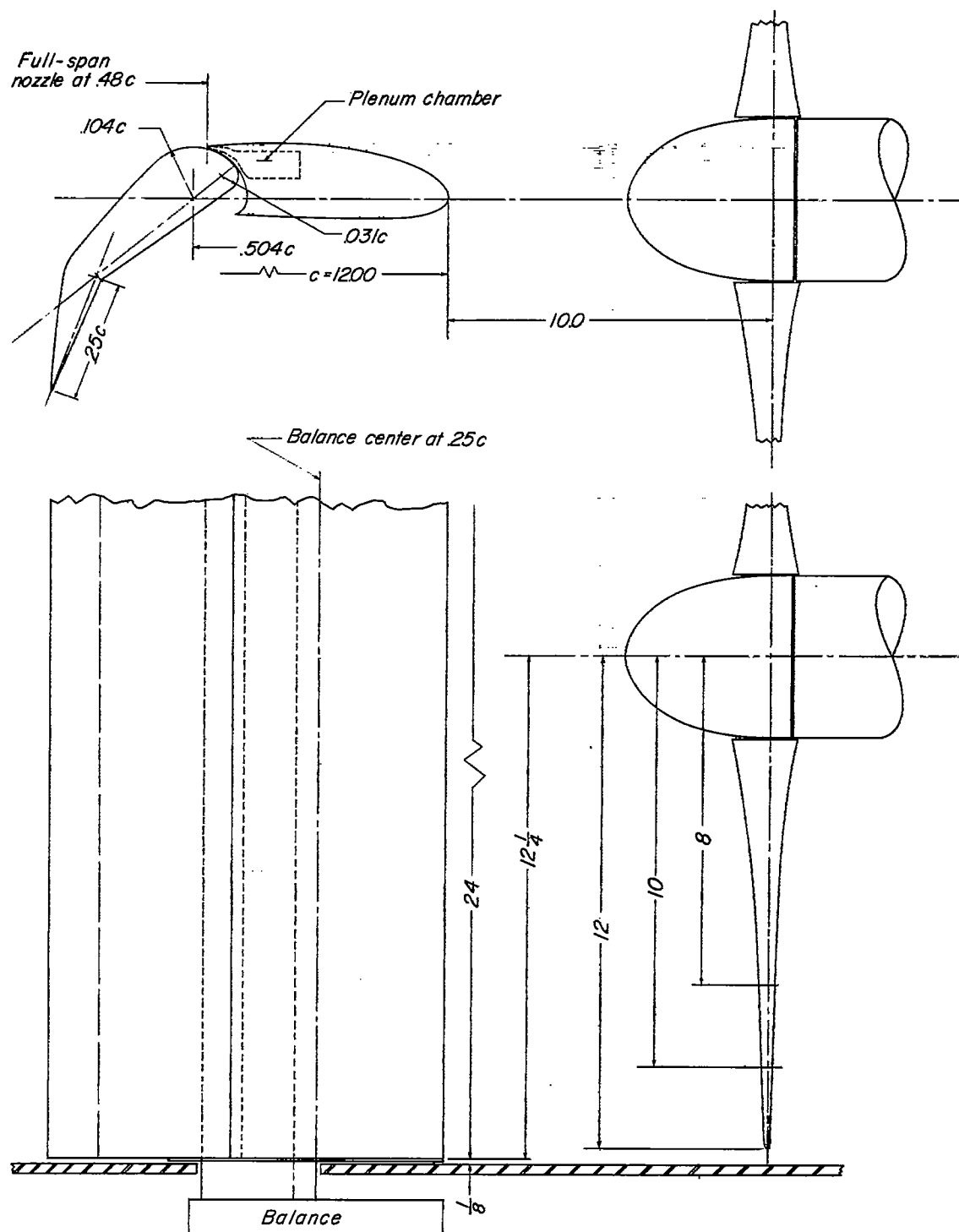
Figure 2.- Drawing of model. Dimensions are in inches unless
otherwise indicated.
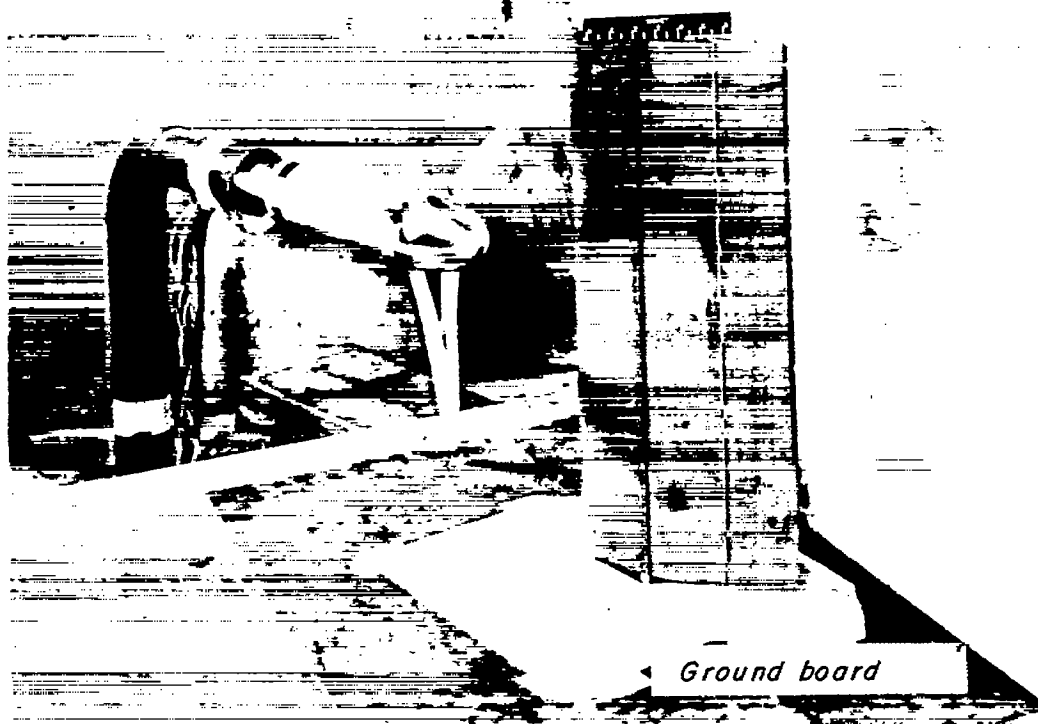
Ground board

L-93296.1

Figure 3.- Model installed on static-thrust stand. Ground board at
h/D ≈ 0.11; 24-inch-diameter propeller.
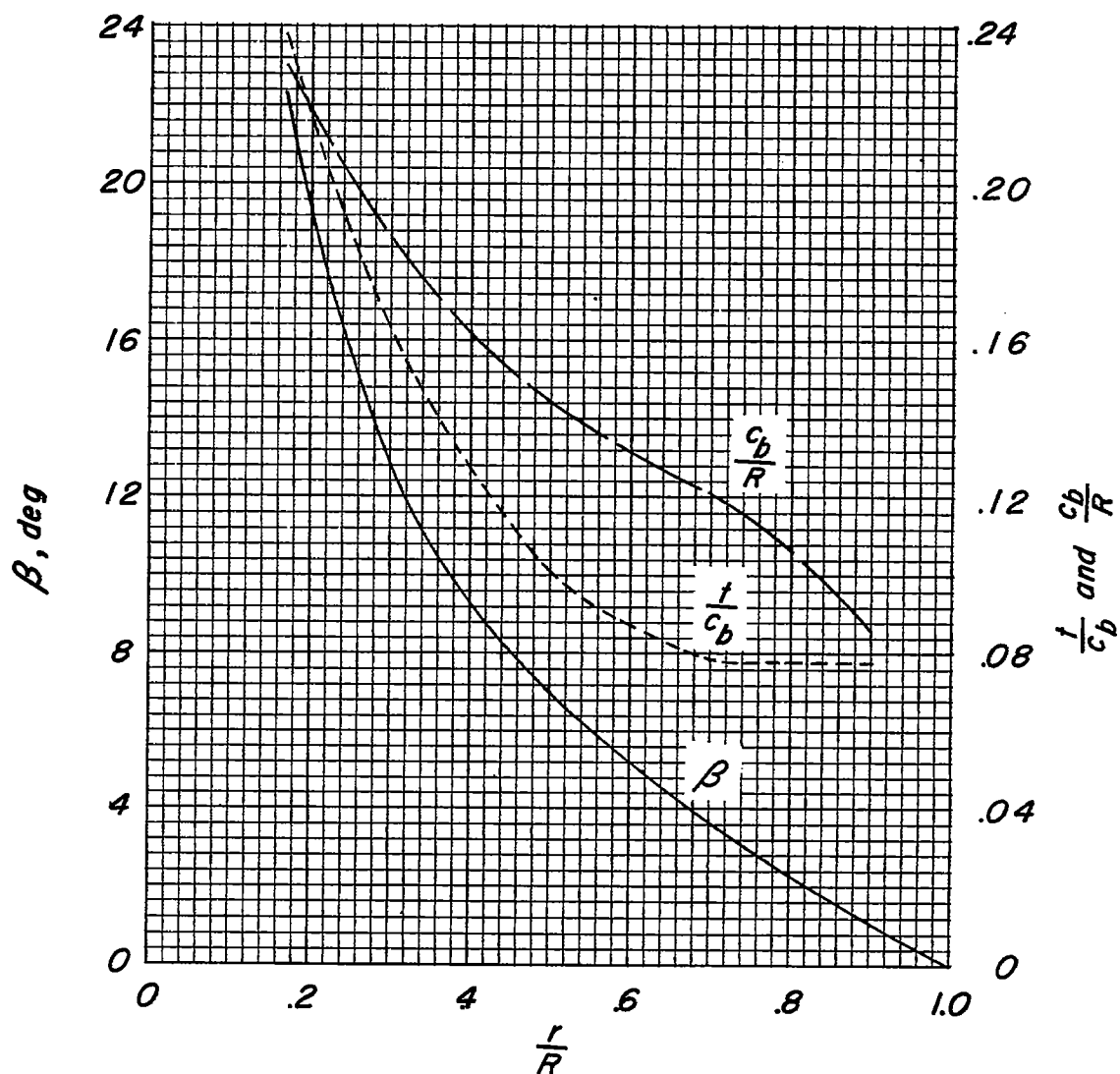
Figure 4.- Physical characteristics of 2-foot-diameter propeller with Clark Y airfoil section. $\eta = 0.60$.
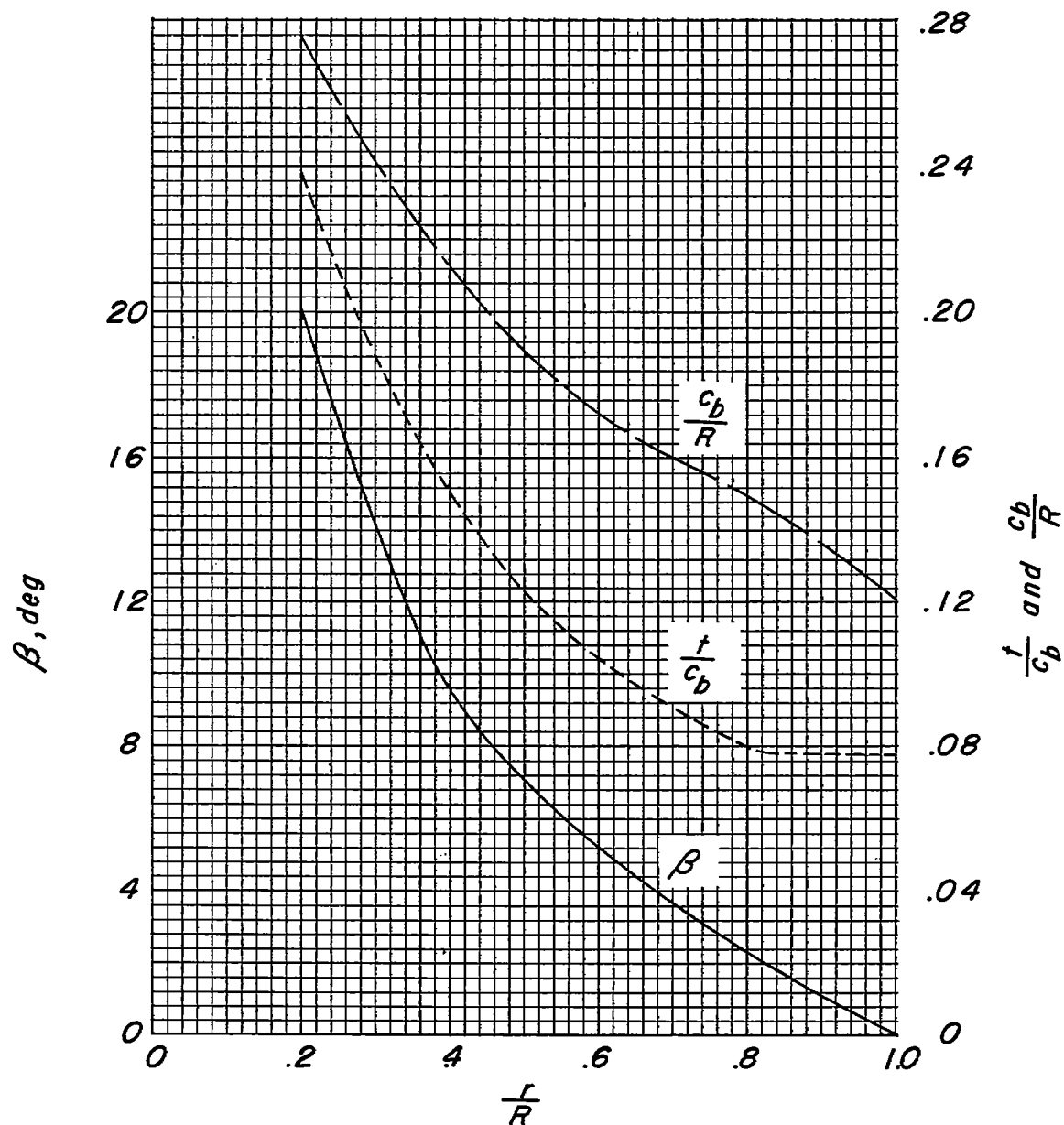
Figure 5.- Physical characteristics of 1.67-foot-diameter propeller
with Clark Y airfoil section. $\eta = 0.66$.
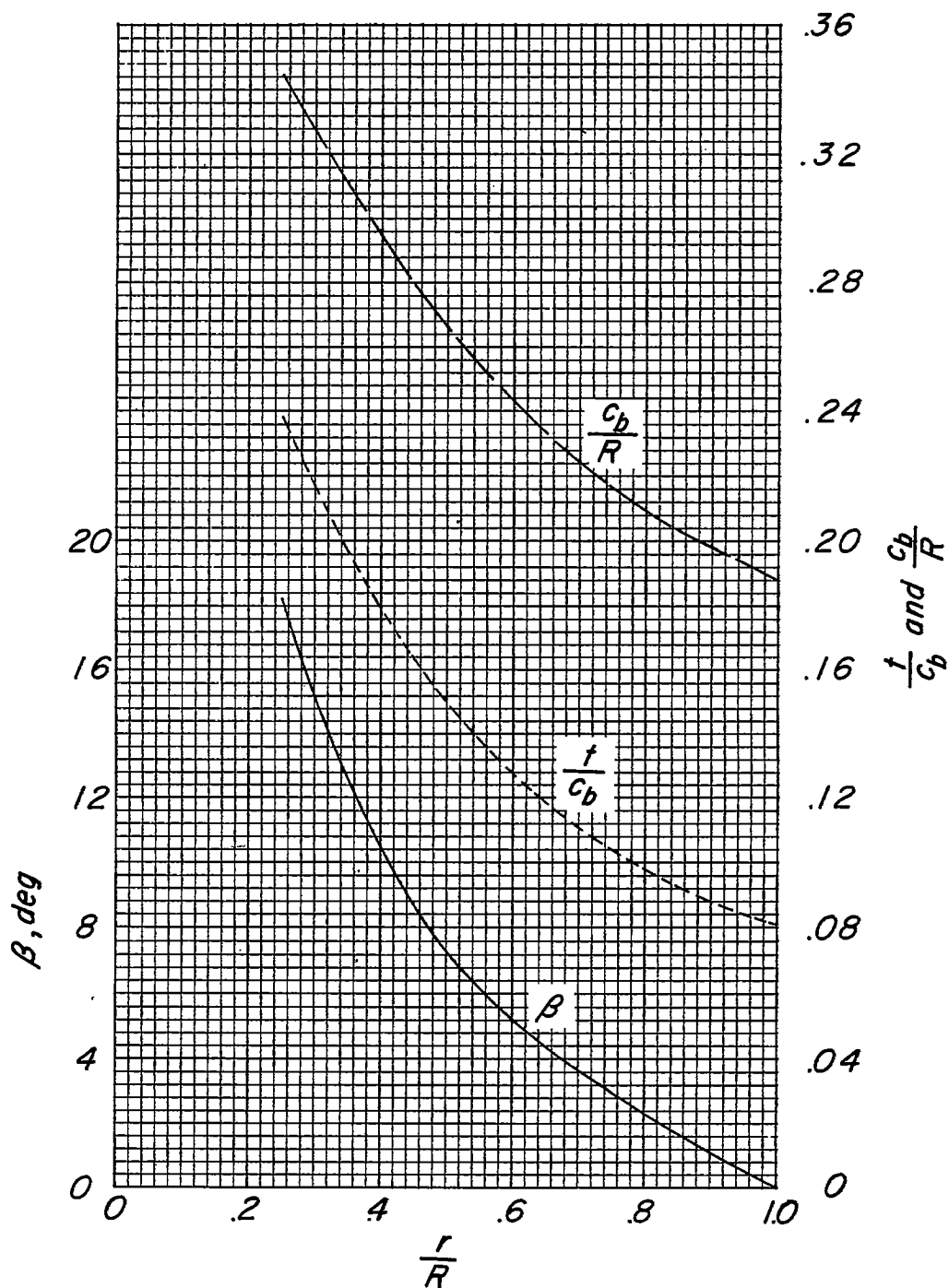
Figure 6.- Physical characteristics of 1.33-foot-diameter propeller
with Clark Y airfoil section. $\eta = 0.62$.
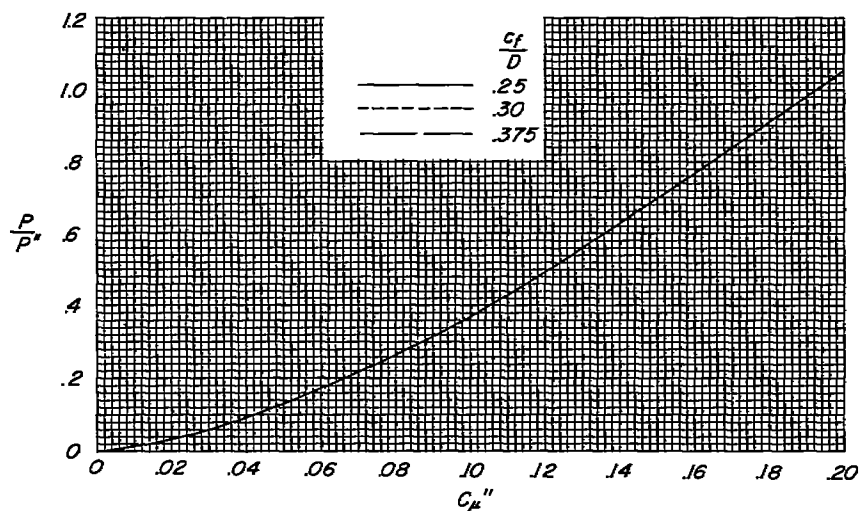
(a) Ratio of power in blowing system to power in slipstream.
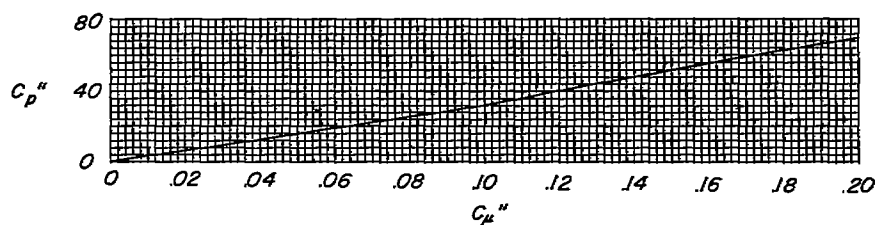
(b) Pressure coefficient.
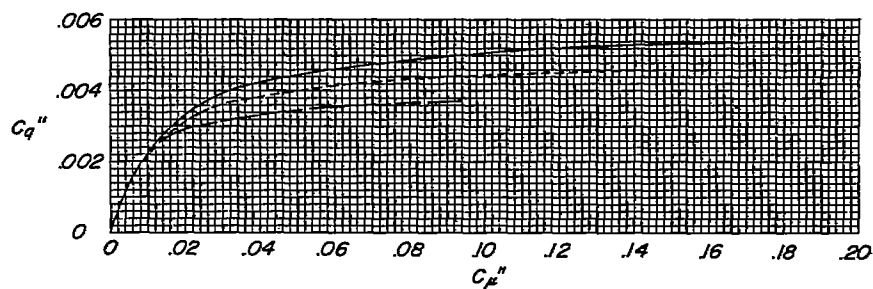
(c) Flow coefficient.

Figure 7.- Variation of ratio of power in blowing system to power in slipstream, pressure coefficient, and flow coefficient with momentum coefficient for the three propeller sizes. Effective nozzle gap, approximately 0.017 inch.
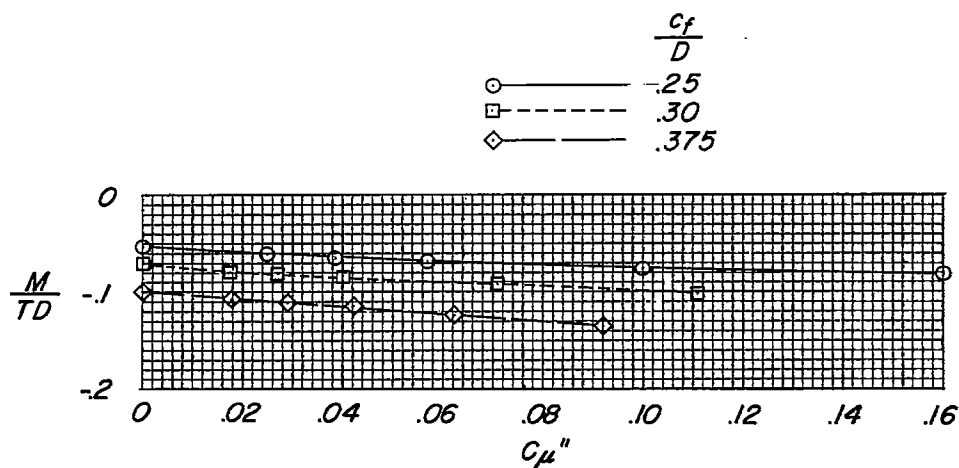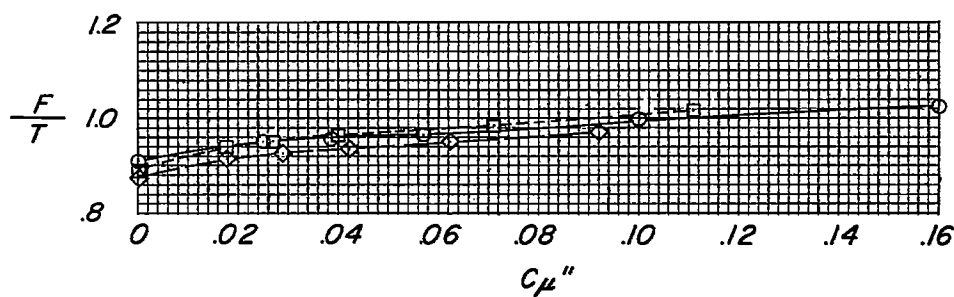
$$\frac{c_f}{D}$$

⊙———— .25
▢————— .30
◇——— .375

(a) Pitching moment as a function of momentum coefficient.

(b) Ratio of resultant force to thrust as a function of momentum coefficient.
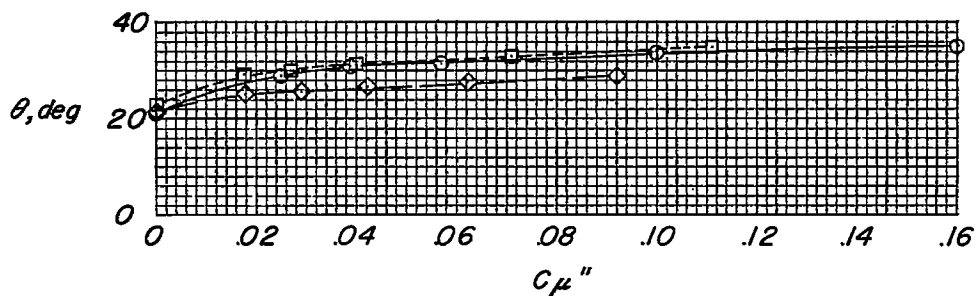
(c) Turning angle as a function of momentum coefficient.

Figure 8.- Effect of ratio of flap chord to propeller diameter on the model characteristics. $\delta_{f,1} = 40°$; $\delta_{f,2} = 0°$; $h/D \approx \infty$.
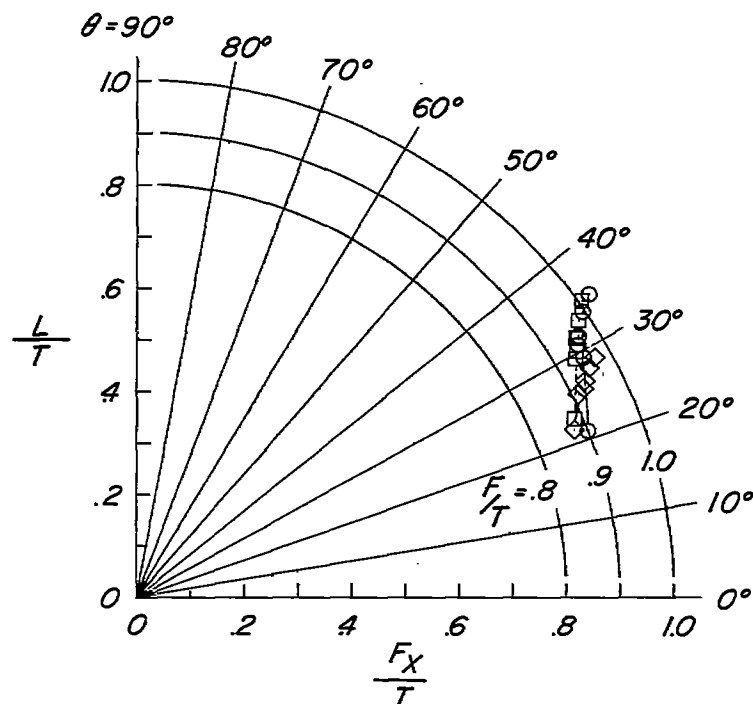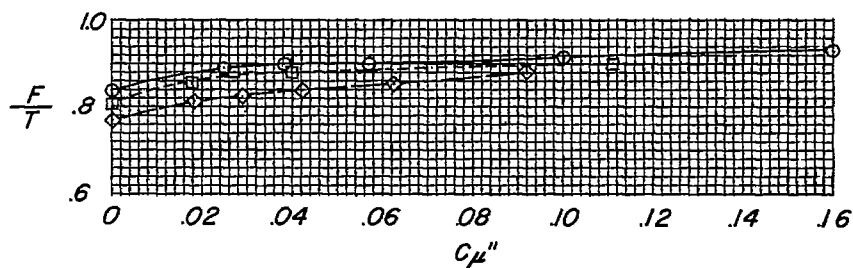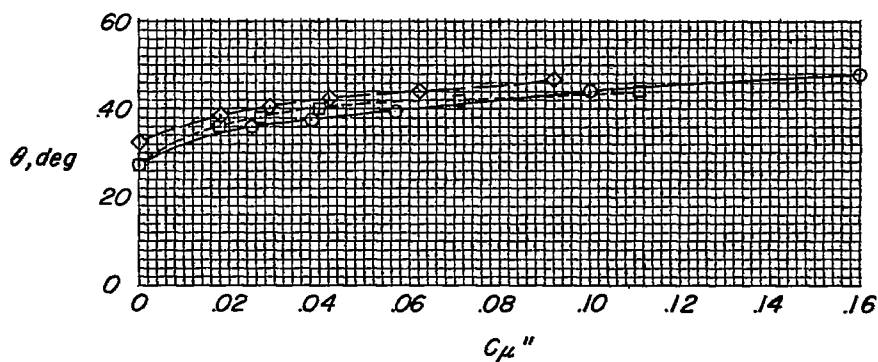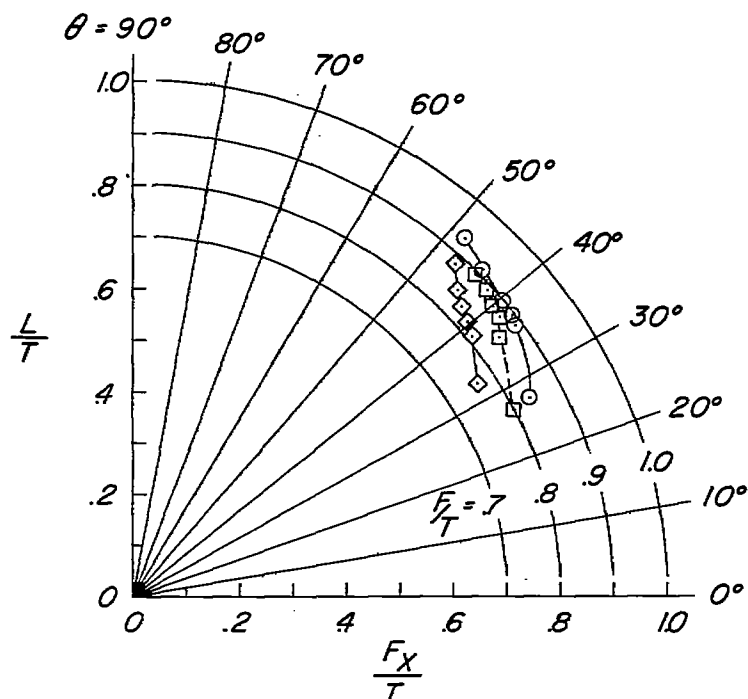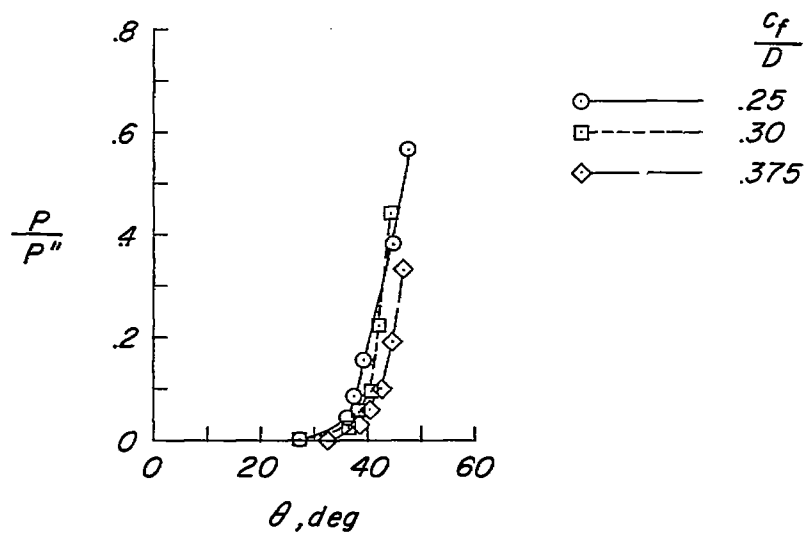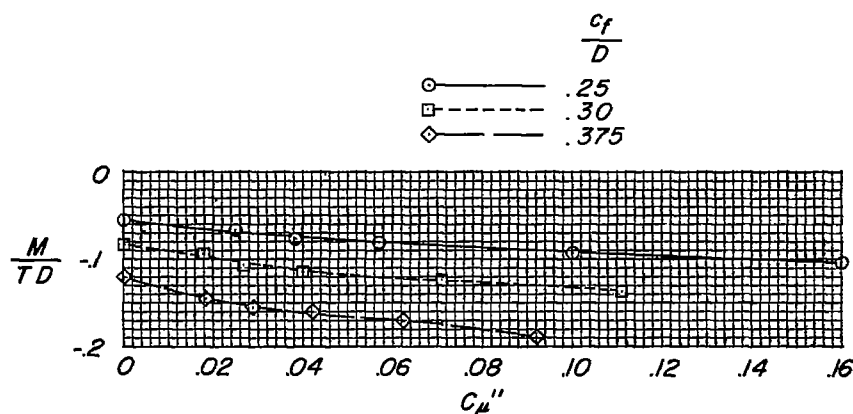
(d) Summary of turning effectiveness.
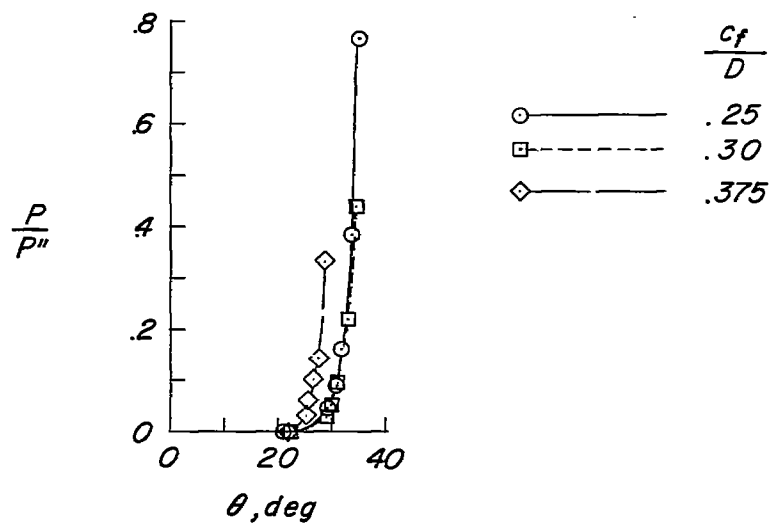
(e) Ratio of power in blowing system to power in slipstream as a
function of turning angle.

Figure 8.- Concluded.
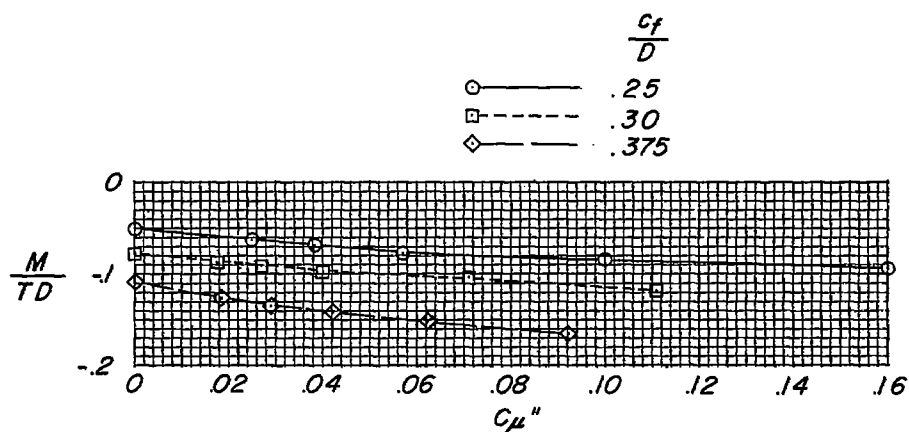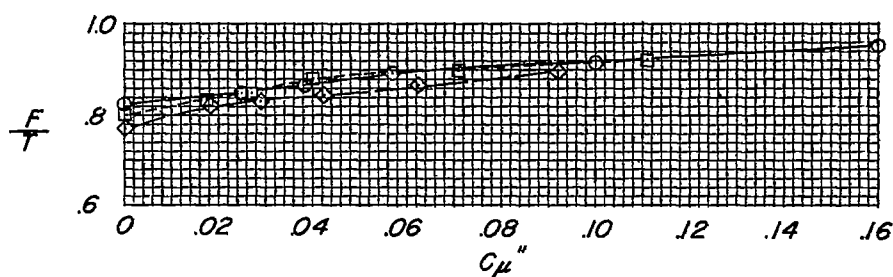
$$\frac{c_f}{D}$$

◦——— .25
□----- .30
◇—·— .375

(a) Pitching moment as a function of momentum coefficient.

(b) Ratio of resultant force to thrust as a function of momentum coefficient.
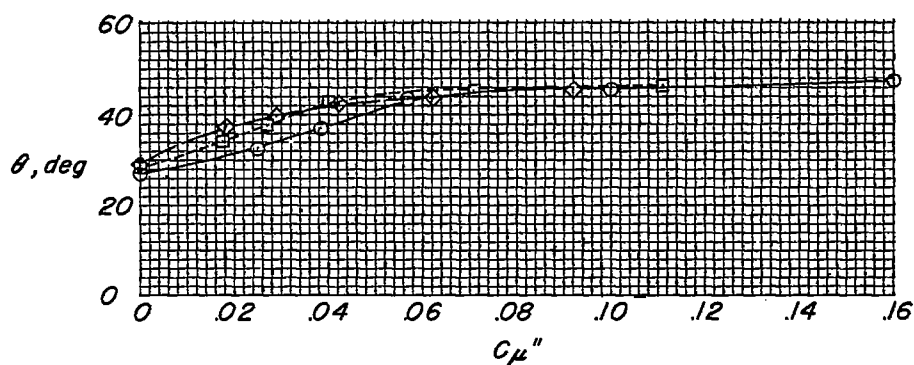
(c) Turning angle as a function of momentum coefficient.

Figure 9.- Effect of ratio of flap chord to propeller diameter on the model characteristics. $\delta_{f,1} = 60^{\circ}$; $\delta_{f,2} = 0^{\circ}$; $h/D \approx \infty$.
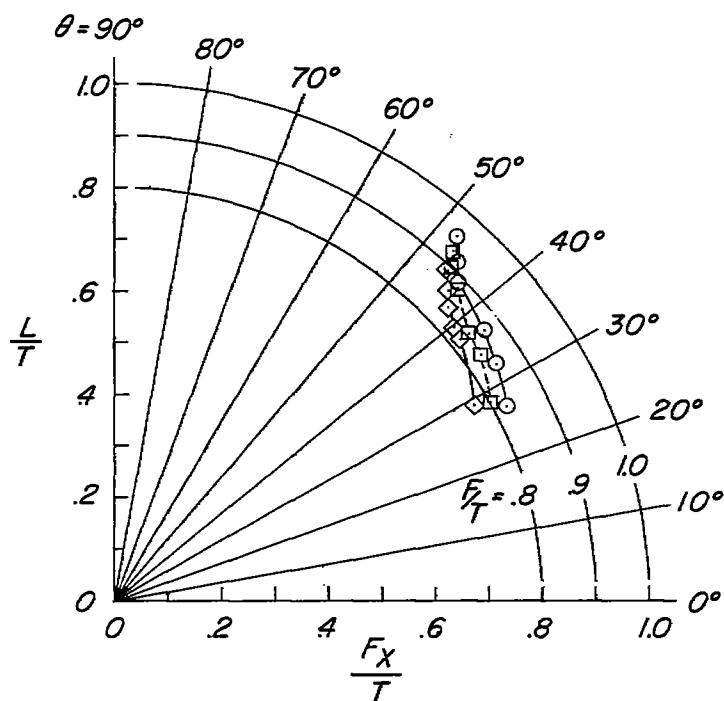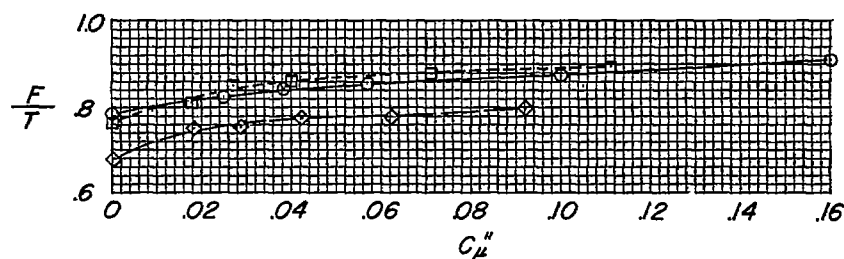
(d) Summary of turning effectiveness.
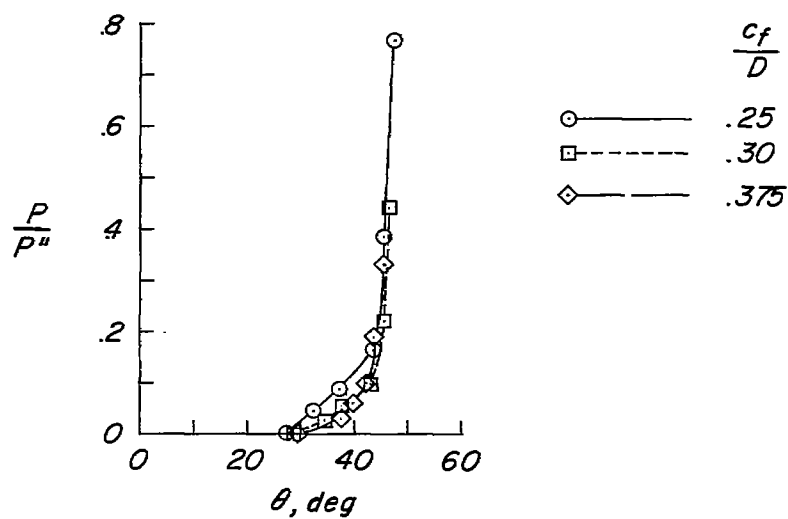
(e) Ratio of power in blowing system to power in slipstream as a
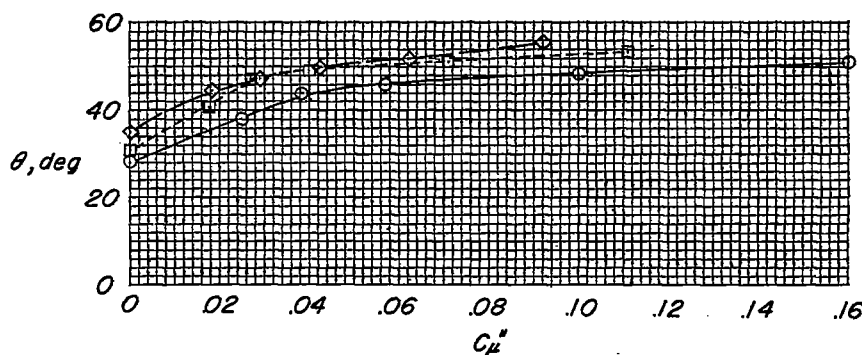function of turning angle.

Figure 9.- Concluded.
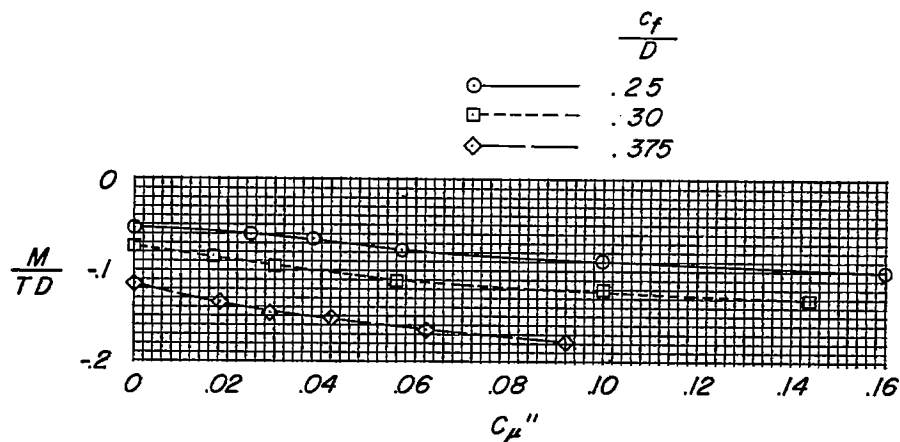
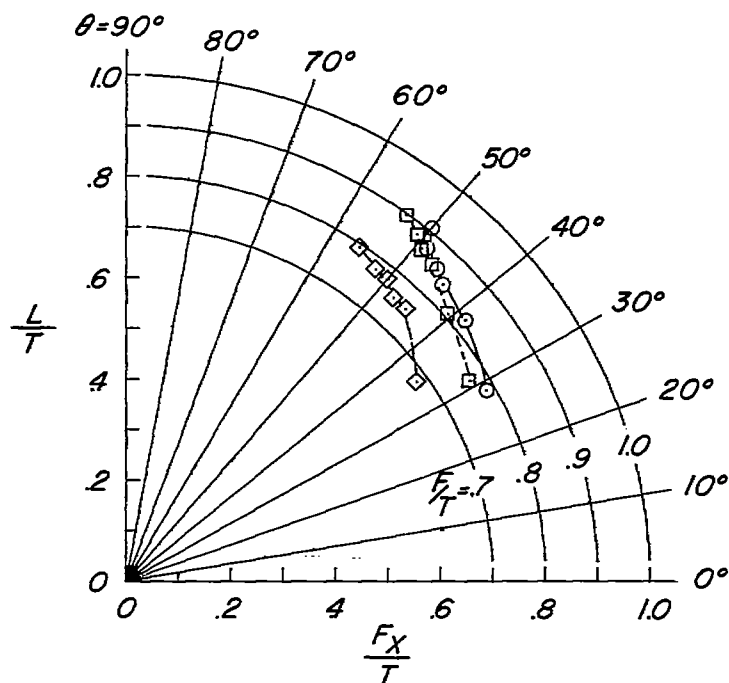(a) Pitching moment as a function of momentum coefficient.
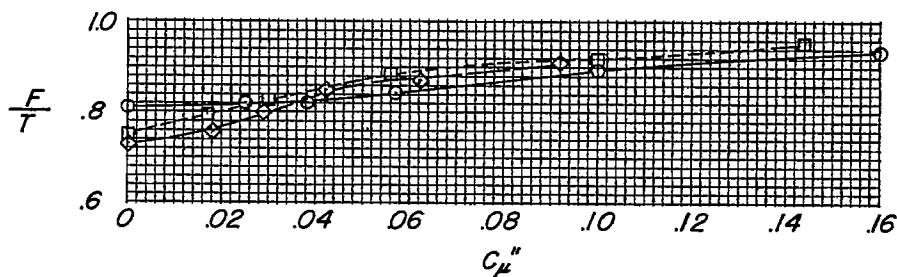
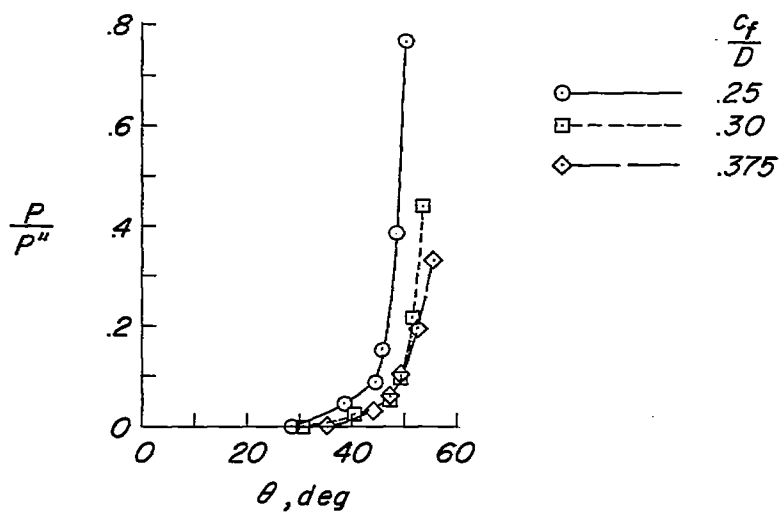(b) Ratio of resultant force to thrust as a function of momentum coefficient.
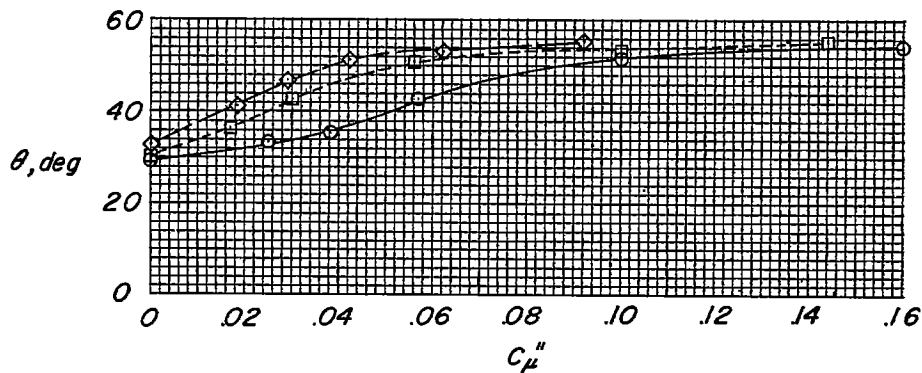
(c) Turning angle as a function of momentum coefficient.

Figure 10.- Effect of ratio of flap chord to propeller diameter on the model characteristics. $\delta_{f,1} = 70°$; $\delta_{f,2} = 0°$; $h/D \approx \infty$.
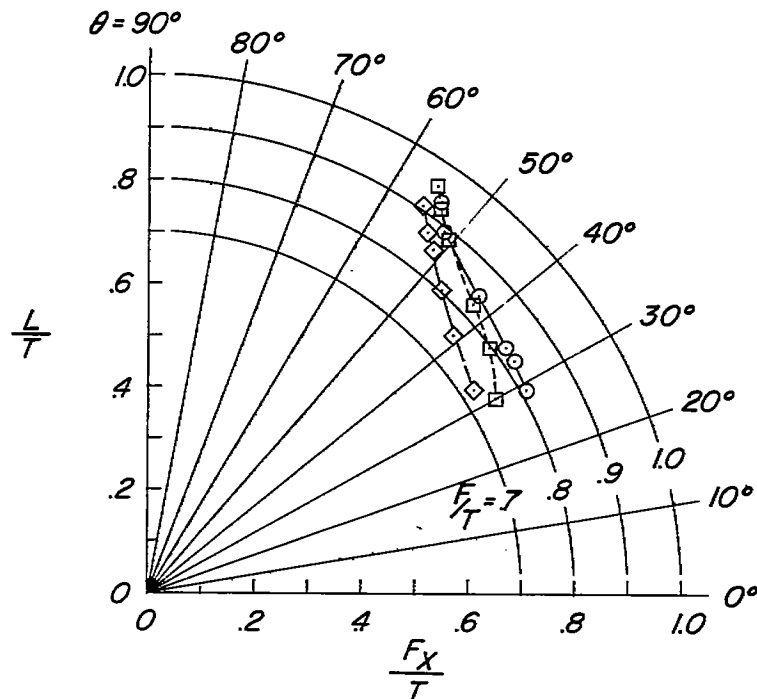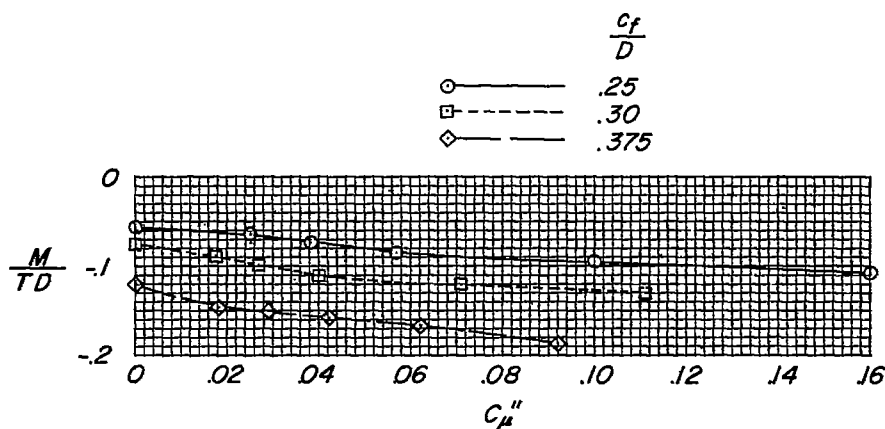
(d) Summary of turning effectiveness.
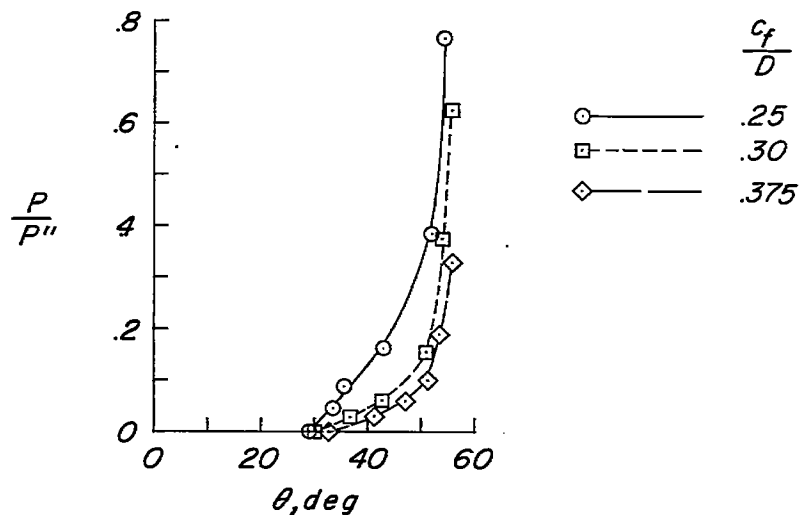
(e) Ratio of power in blowing system to power in slipstream as a
function of turning angle.

Figure 10.- Concluded.
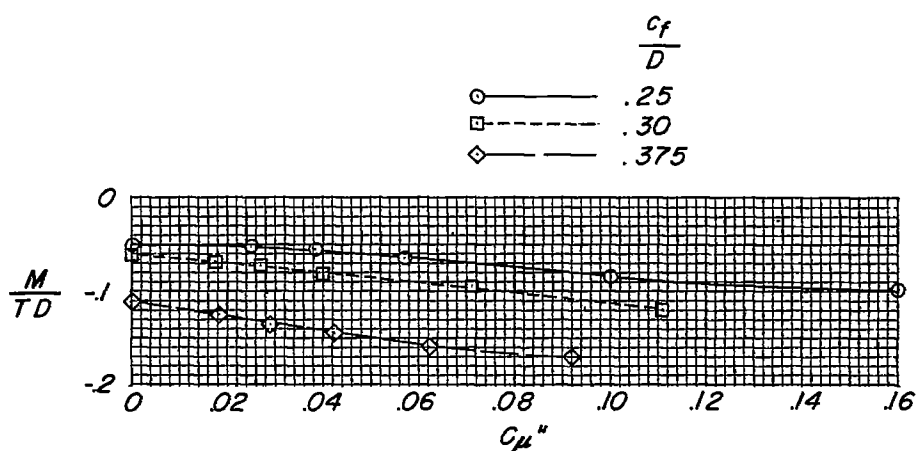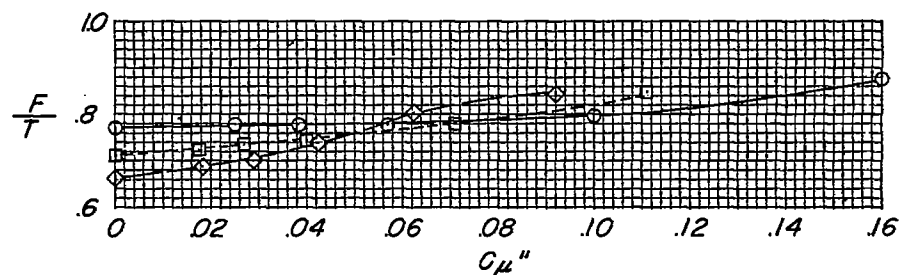
$$\frac{c_f}{D}$$

⊙———— .25
⊡------ .30
◇——— .375

(a) Pitching moment as a function of momentum coefficient.

(b) Ratio of resultant force to thrust as a function of momentum
coefficient.
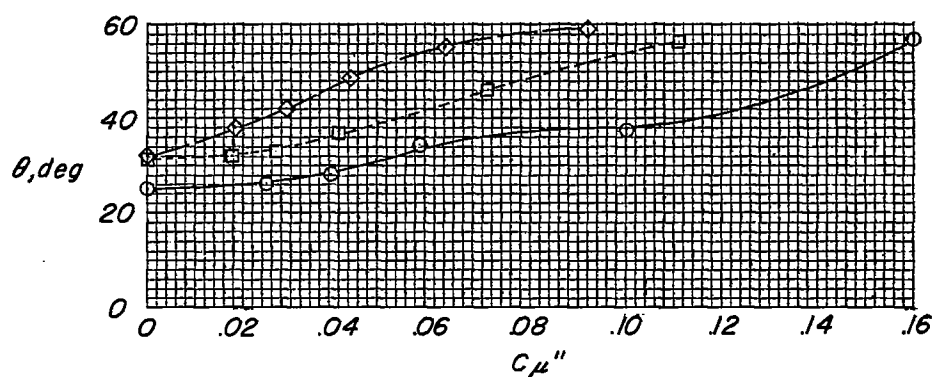
(c) Turning angle as a function of momentum coefficient.

Figure 11.- Effect of ratio of flap chord to propeller diameter on the
model characteristics. $\delta_{f,1} = 80°$; $\delta_{f,2} = 0°$; $h/D \approx \infty$.
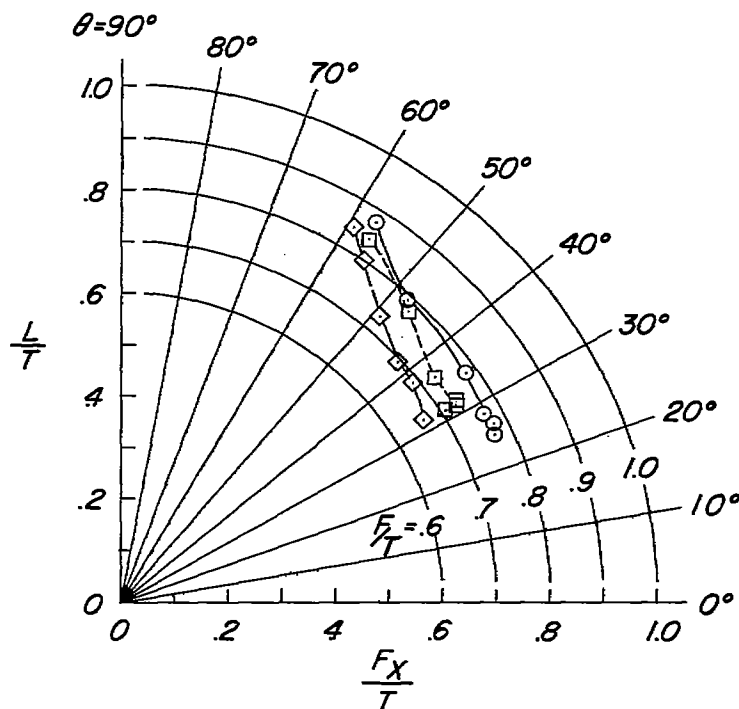
(d) Summary of turning effectiveness.
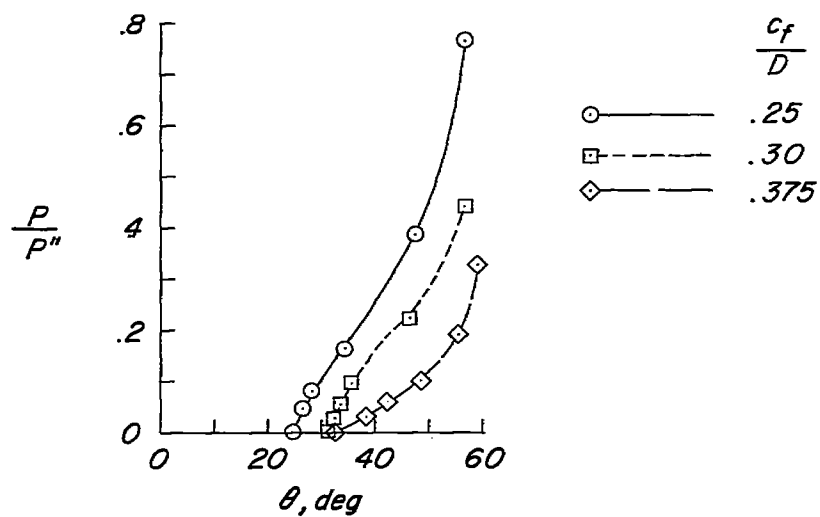
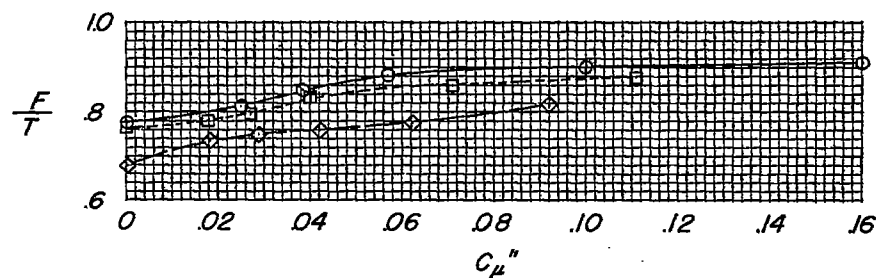(e) Ratio of power in blowing system to power in slipstream as a
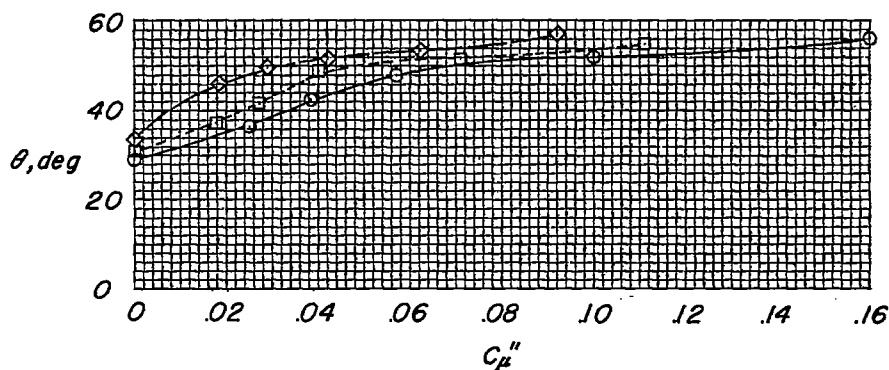function of turning angle.

Figure 11.- Concluded.
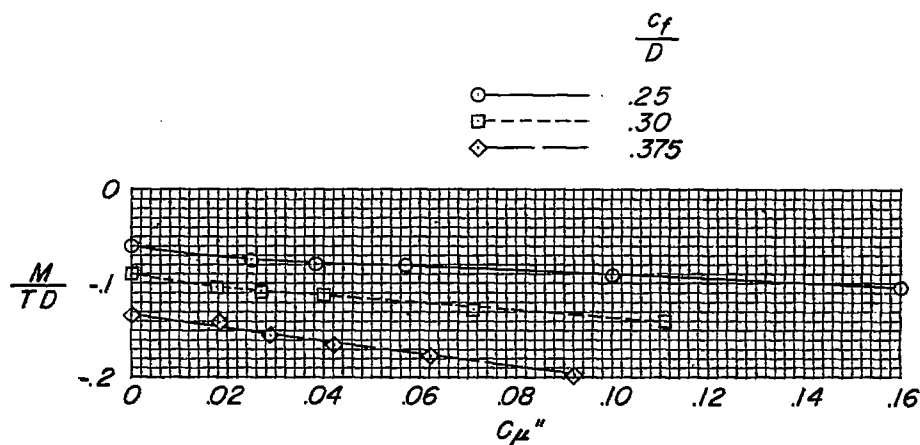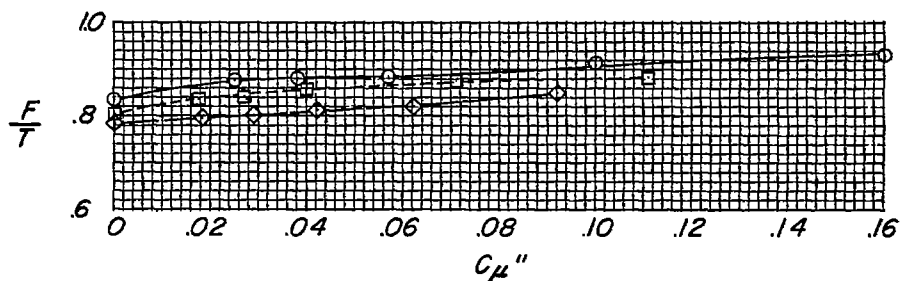
$$\frac{c_f}{D}$$

○———— .25
□——————— .30
◇——— —— .375

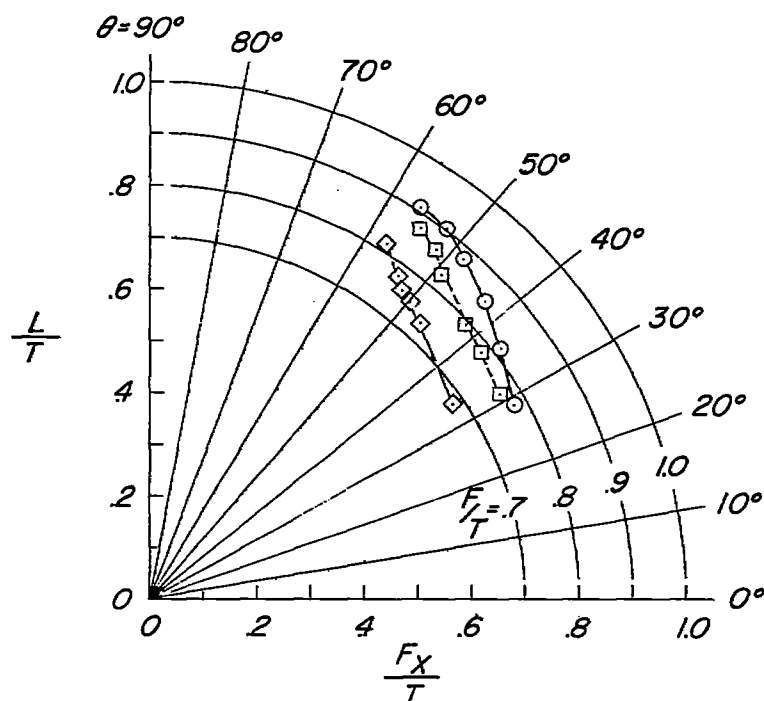(a) Pitching moment as a function of momentum coefficient.

(b) Ratio of resultant force to thrust as a function of momentum coefficient.
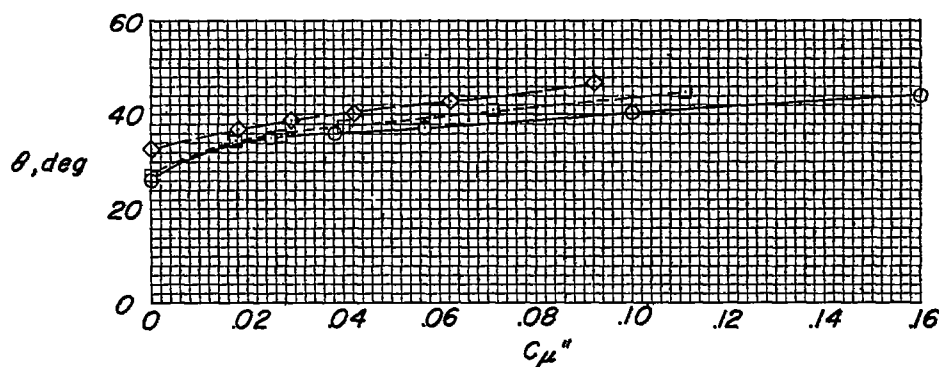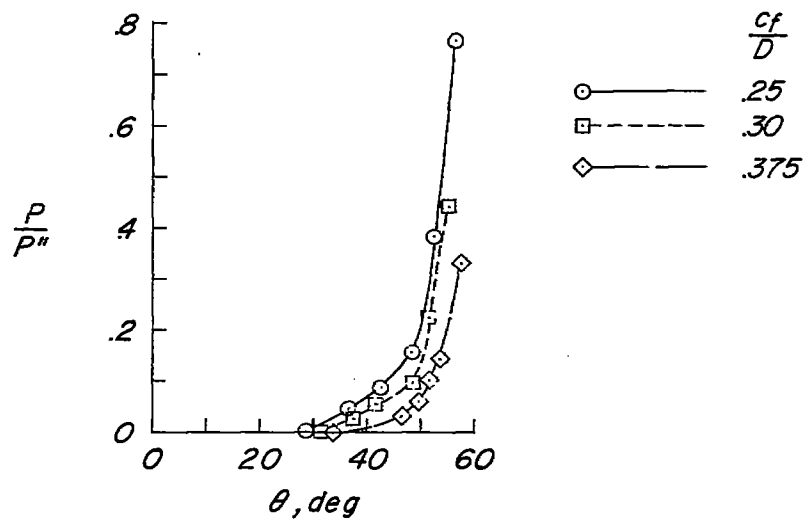

(c) Turning angle as a function of momentum coefficient.

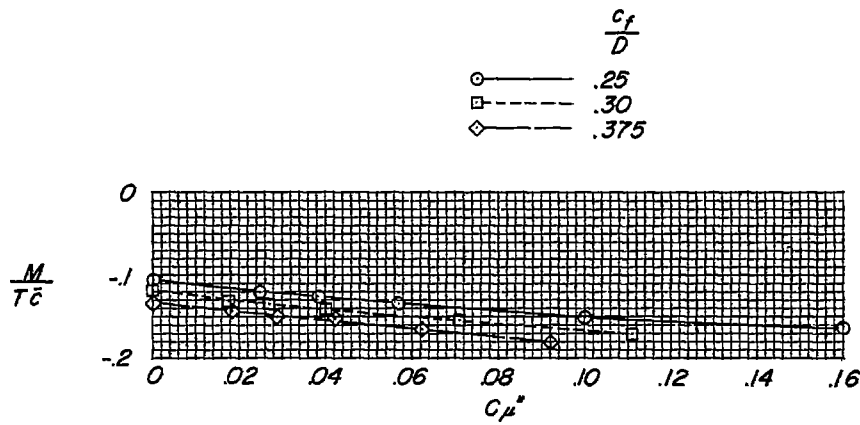Figure 12.- Effect of ratio of flap chord to propeller diameter on the model characteristics. $\delta_{f,1} = 30°$; $\delta_{f,2} = 50°$; $h/D \approx \infty$.
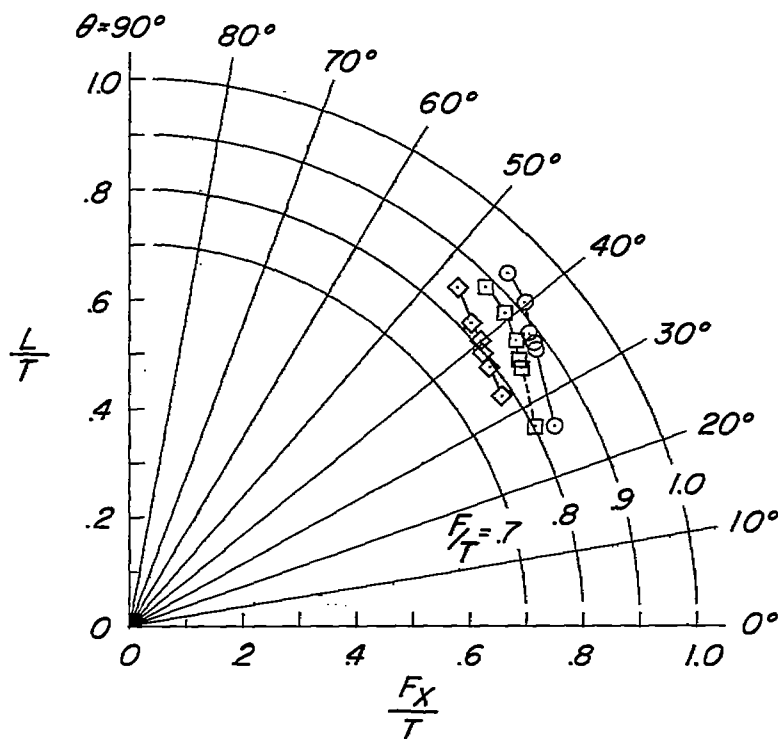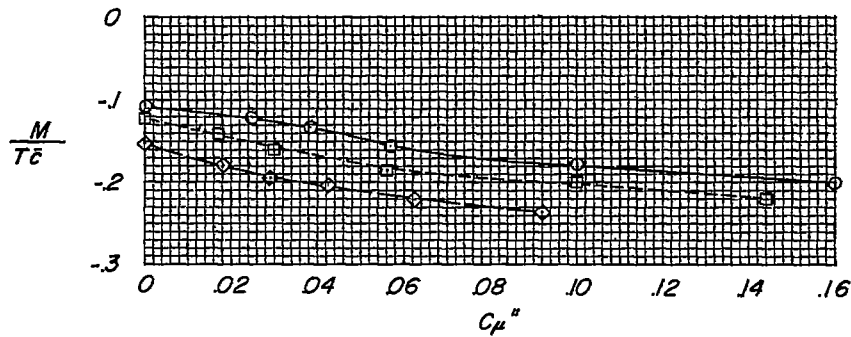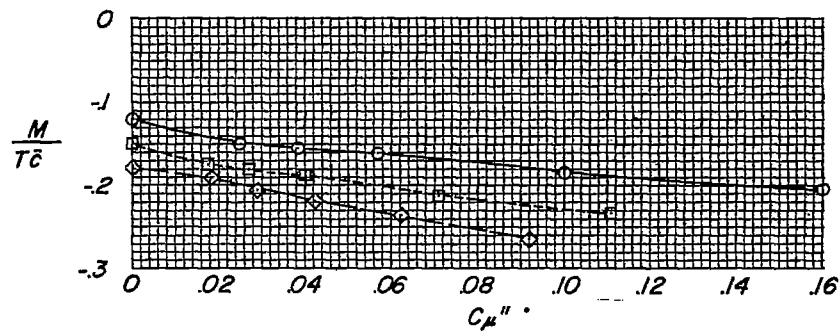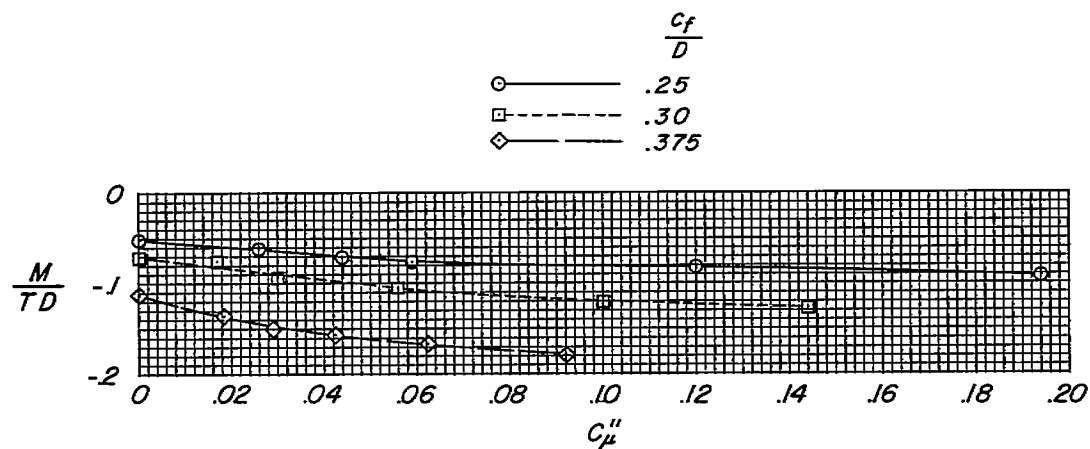
(d) Summary of turning effectiveness.
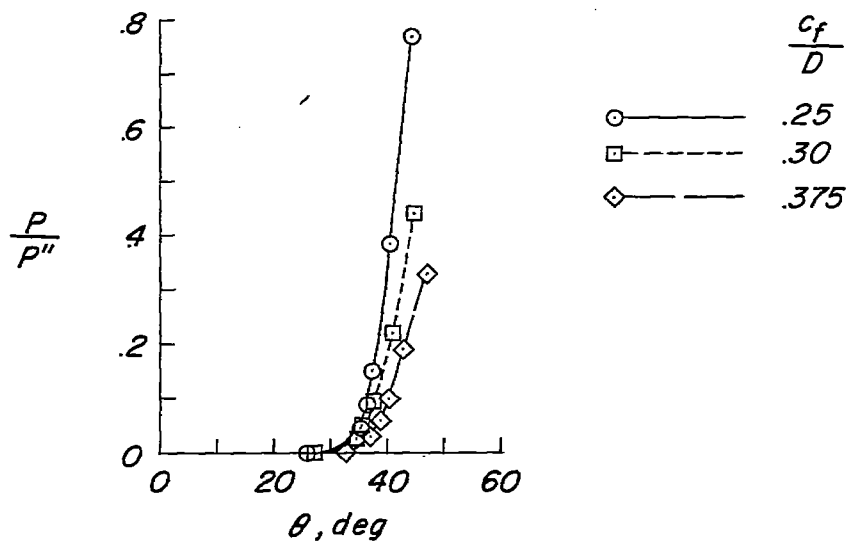
(e) Ratio of power in blowing system to power in slipstream as a function of turning angle.

Figure 12.- Concluded.
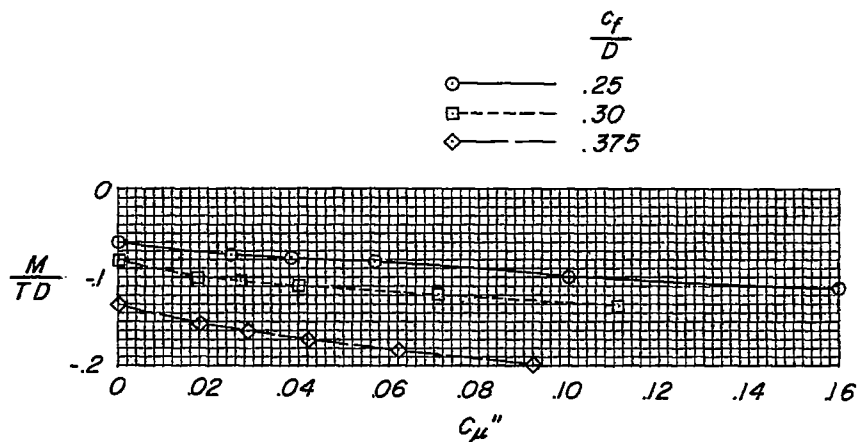
$$\frac{c_f}{D}$$

⊙————	.25
□-----	.30
◇———	.375

(a) Pitching moment as a function of momentum coefficient.

(b) Ratio of resultant force to thrust as a function of momentum coefficient.

(c) Turning angle as a function of momentum coefficient.

Figure 13.- Effect of ratio of flap chord to propeller diameter on the model characteristics. $\delta_{f,1} = 40°$; $\delta_{f,2} = 30°$; $h/D \approx \infty$.
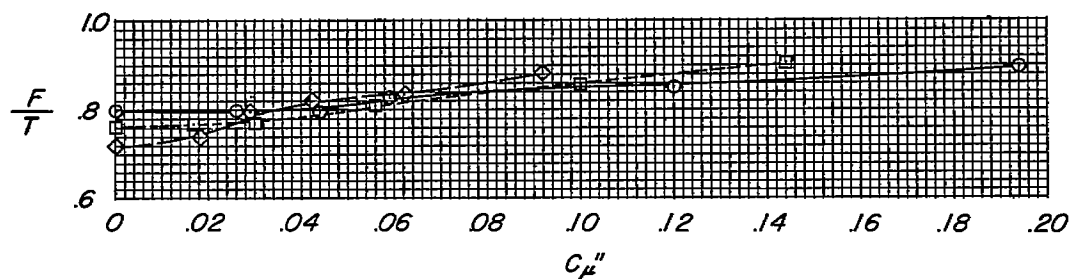
(d) Summary of turning effectiveness.

(e) Ratio of power in blowing system to power in slipstream as a
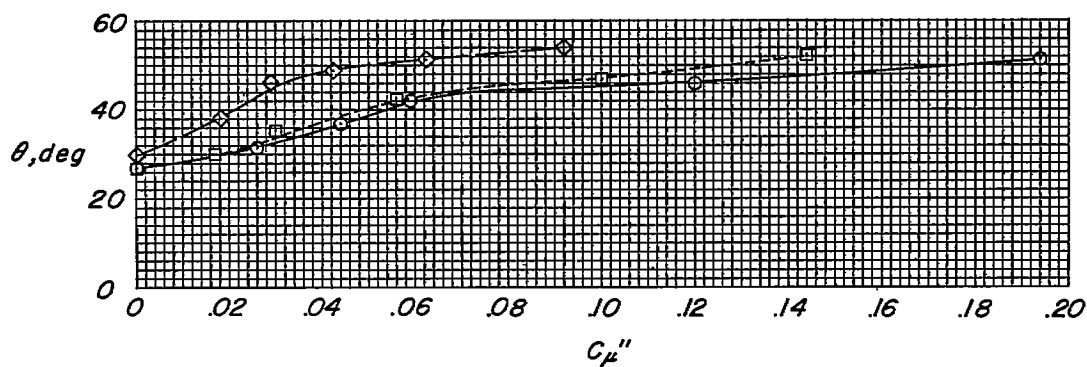function of turning angle.

Figure 13.- Concluded.

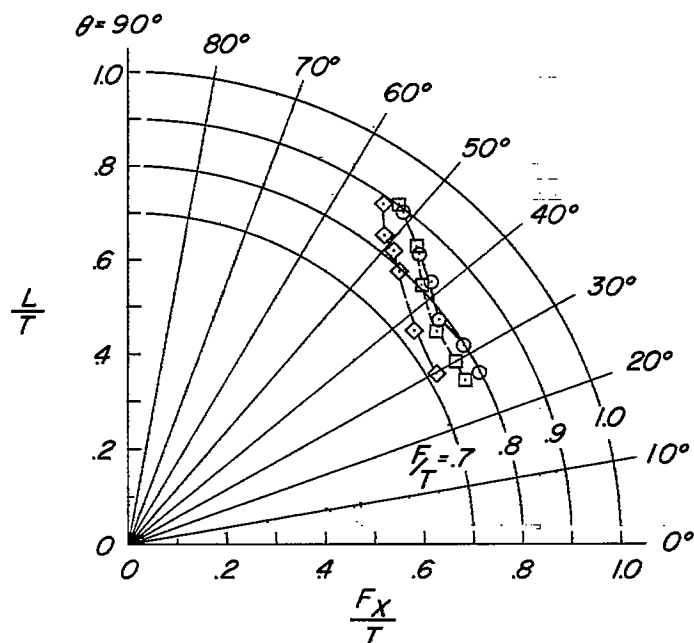(a) Pitching moment as a function of momentum coefficient.

(b) Ratio of resultant force to thrust as a function of momentum coefficient.
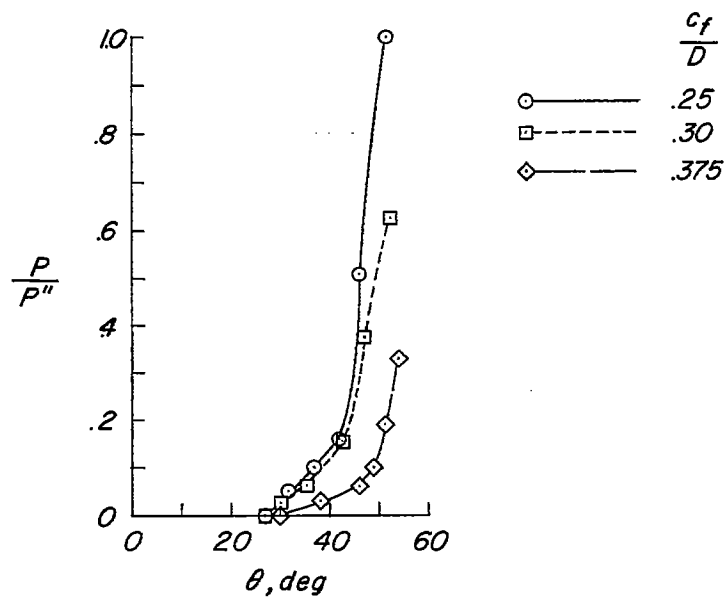

(c) Turning angle as a function of momentum coefficient.

Figure 14.- Effect of ratio of flap chord to propeller diameter on the model characteristics. $\delta_{f,1} = 50°$; $\delta_{f,2} = 40°$; $h/D \approx \infty$.
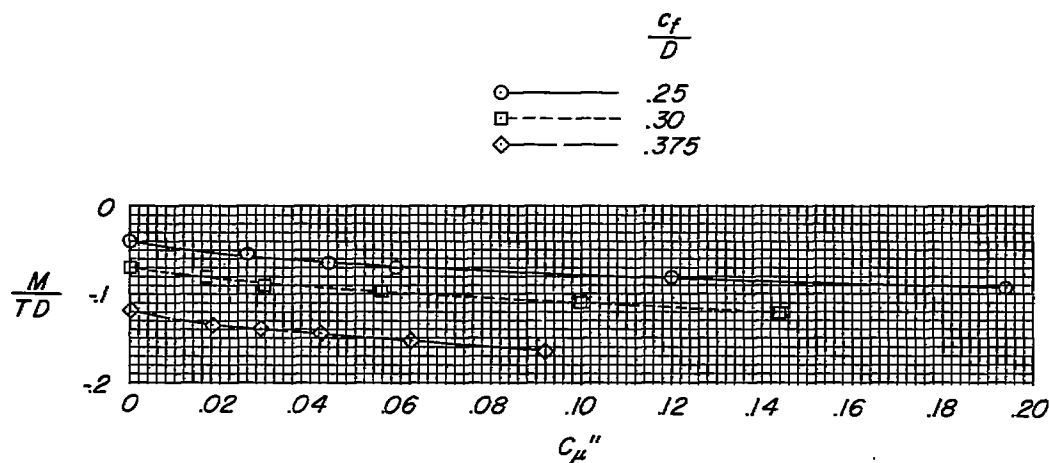
(d) Summary of turning effectiveness.

(e) Ratio of power in blowing system to power in slipstream as a
function of turning angle.

Figure 14.- Concluded.

$$\frac{c_f}{D}$$

○————— .25
□------- .30
◇— — .375

(a) Pitching moment as a function of momentum coefficient.

(b) Ratio of resultant force to thrust as a function of momentum coefficient.

(c) Turning angle as a function of momentum coefficient.

Figure 15.- Effect of ratio of flap chord to propeller diameter on the model characteristics. $\delta_{f,1} = 60°$; $\delta_{f,2} = 30°$; $h/D \approx \infty$.
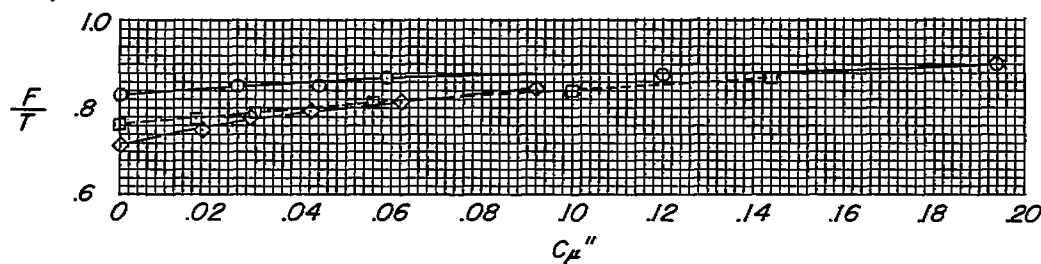
(d) Summary of turning effectiveness.

(e) Ratio of power in blowing system to power in slipstream as a
function of turning angle.

Figure 15.- Concluded.

$$\frac{c_f}{D}$$

○————— .25
□— — — .30
◇— · — · .375

(a) $\delta_{f,1} = 40^{\circ}$; $\delta_{f,2} = 0^{\circ}$.

(b) $\delta_{f,1} = 70^{\circ}$; $\delta_{f,2} = 0^{\circ}$.

(c) $\delta_{f,1} = 30^{\circ}$; $\delta_{f,2} = 50^{\circ}$.

Figure 16.- Effect of ratio of flap chord to propeller diameter on
moments based on $\bar{c}$. $h/D \approx \infty$.

$$\frac{c_f}{D}$$

○─────── .25
□─────── .30
◇─────── .375

(a) Pitching moment as a function of momentum coefficient.

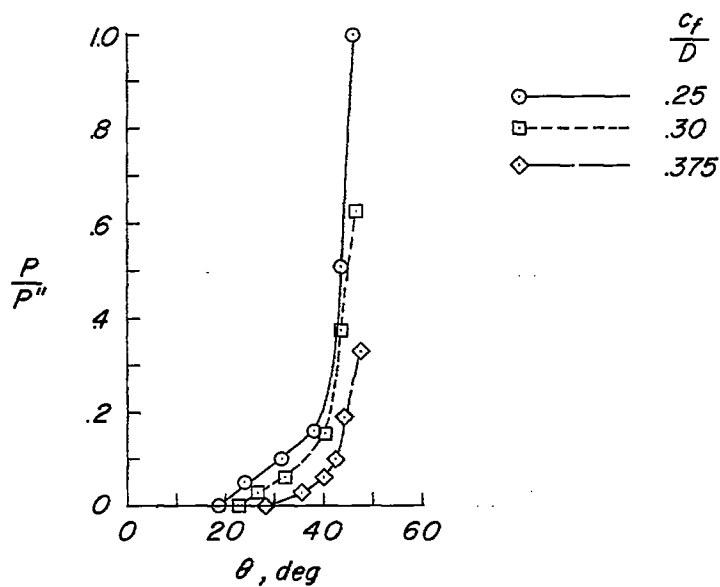(b) Ratio of resultant force to thrust as a function of momentum coefficient.

(c) Turning angle as a function of momentum coefficient.

Figure 17.- Effect of ratio of flap chord to propeller diameter on the model characteristics. $\delta_{f,1} = 70°$; $\delta_{f,2} = 0°$; $h = 2.21$ feet.
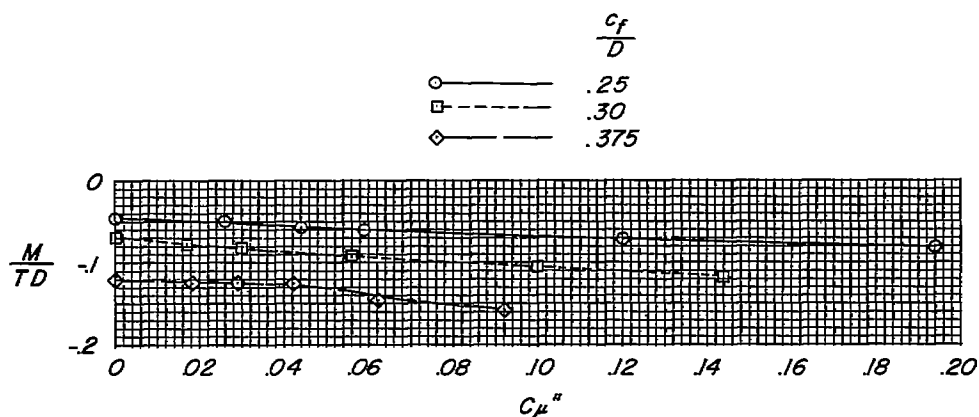
(d) Summary of turning effectiveness.

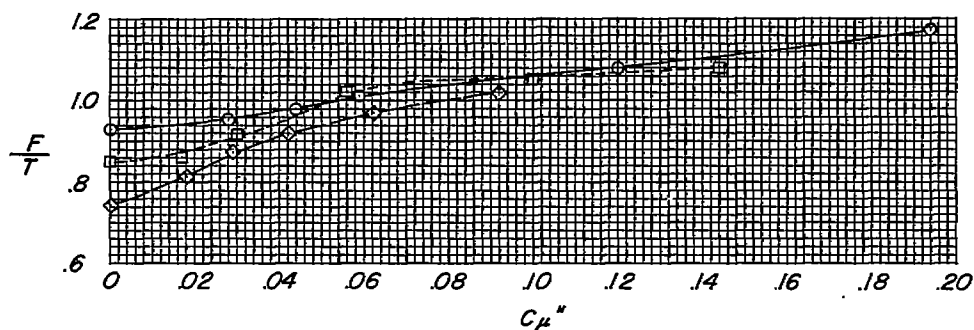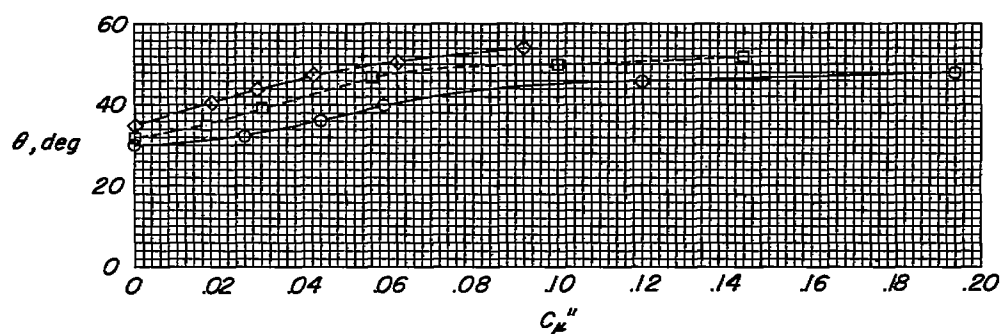(e) Ratio of power in blowing system to power in slipstream as a
function of turning angle.

Figure 17.- Concluded.

$$\frac{c_f}{D}$$

⊙————	.25
▢-------	.30
◇—— ——	.375

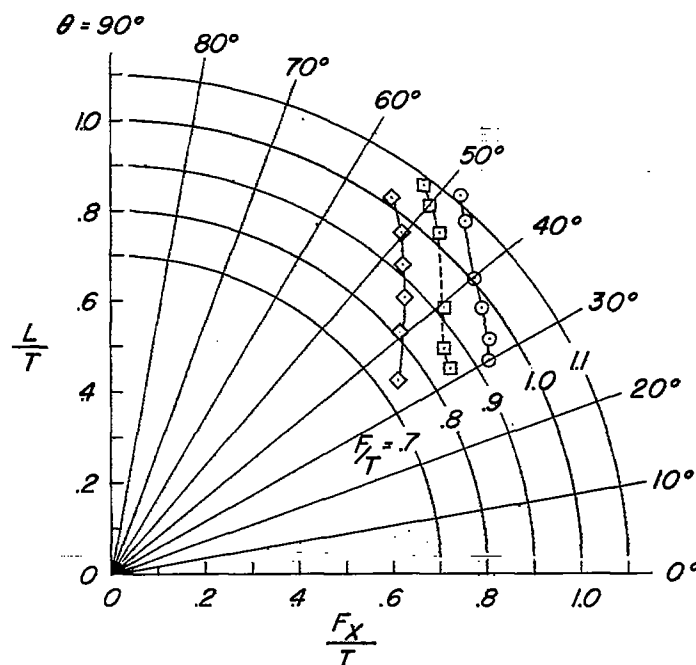(a) Pitching moment as a function of momentum coefficient.

(b) Ratio of resultant force to thrust as a function of momentum coefficient.
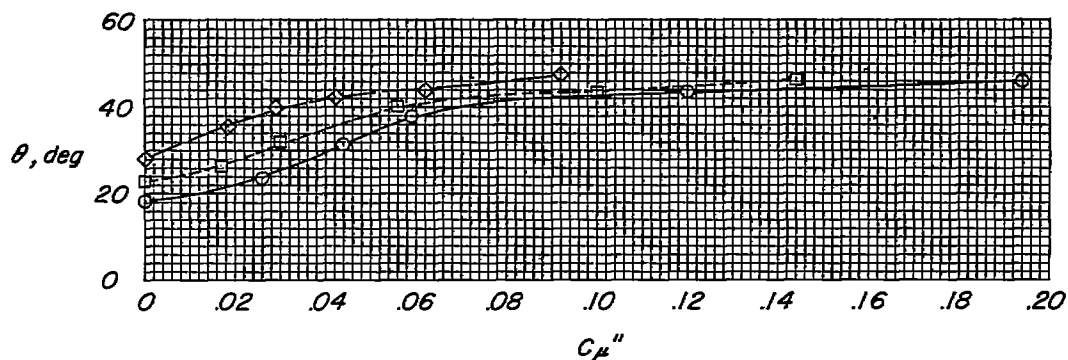
(c) Turning angle as a function of momentum coefficient.

Figure 18.- Effect of ratio of flap chord to propeller diameter on the model characteristics. $\delta_{f,1} = 70°$; $\delta_{f,2} = 0°$; h = 0.71 foot.
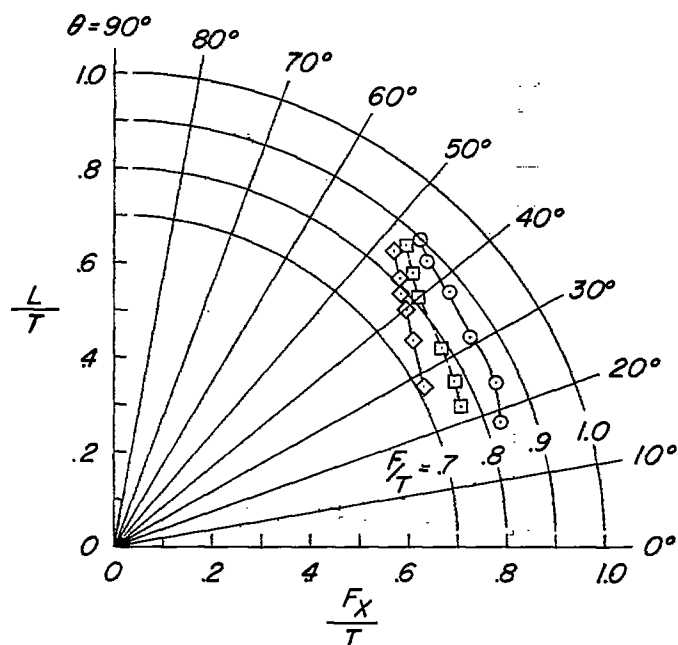
(d) Summary of turning effectiveness.

(e) Ratio of power in blowing system to power in slipstream as a
function of turning angle.

Figure 18.- Concluded.

(a) Pitching moment as a function of momentum coefficient.

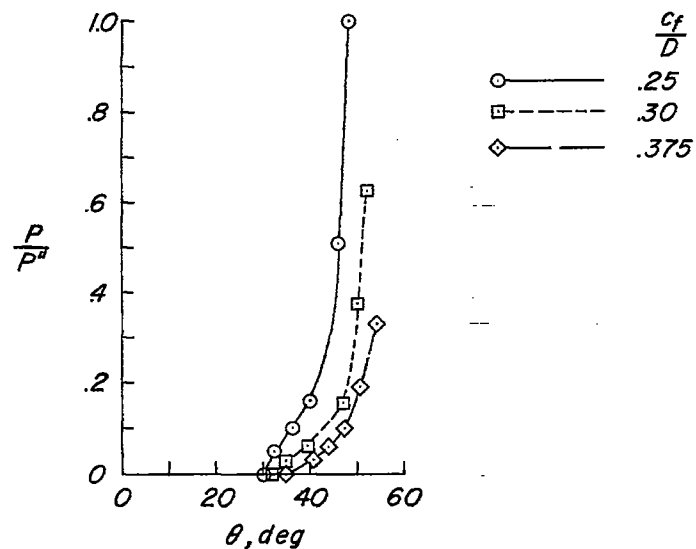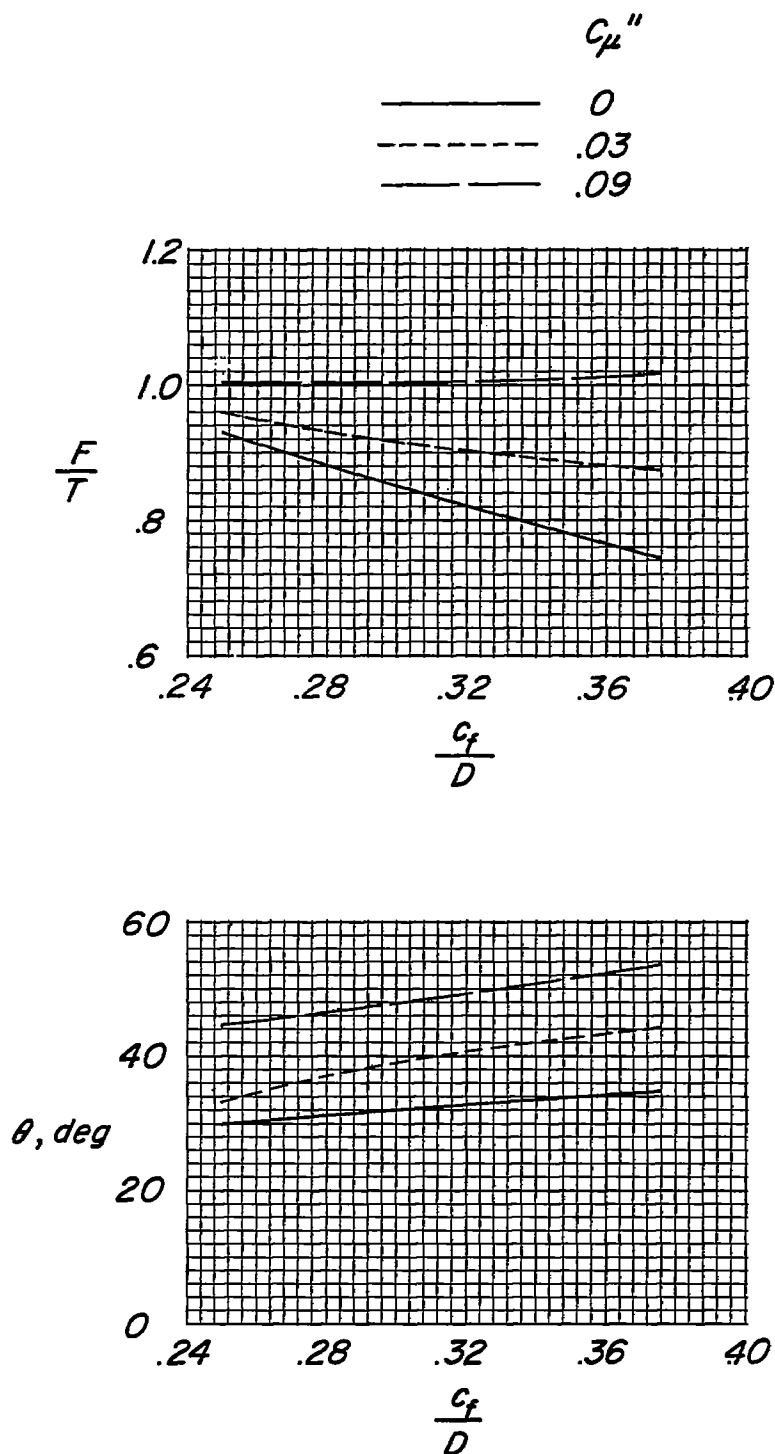(b) Ratio of resultant force to thrust as a function of momentum coefficient.

(c) Turning angle as a function of momentum coefficient.

Figure 19.- Effect of ratio of flap chord to propeller diameter on the model characteristics. $\delta_{f,1} = 70°$; $\delta_{f,2} = 0°$; h = 0.21 foot.

(d) Summary of turning effectiveness.

(e) Ratio of power in blowing system to power in slipstream as a
function of turning angle.

Figure 19.- Concluded.

Figure 20.- Effect of ratio of flap chord to propeller diameter on the ratio of resultant force to thrust and turning angle for a range of momentum coefficients. $\delta_{f,1} = 70^\circ$; $\delta_{f,2} = 0^\circ$; $h = 0.21$ foot.
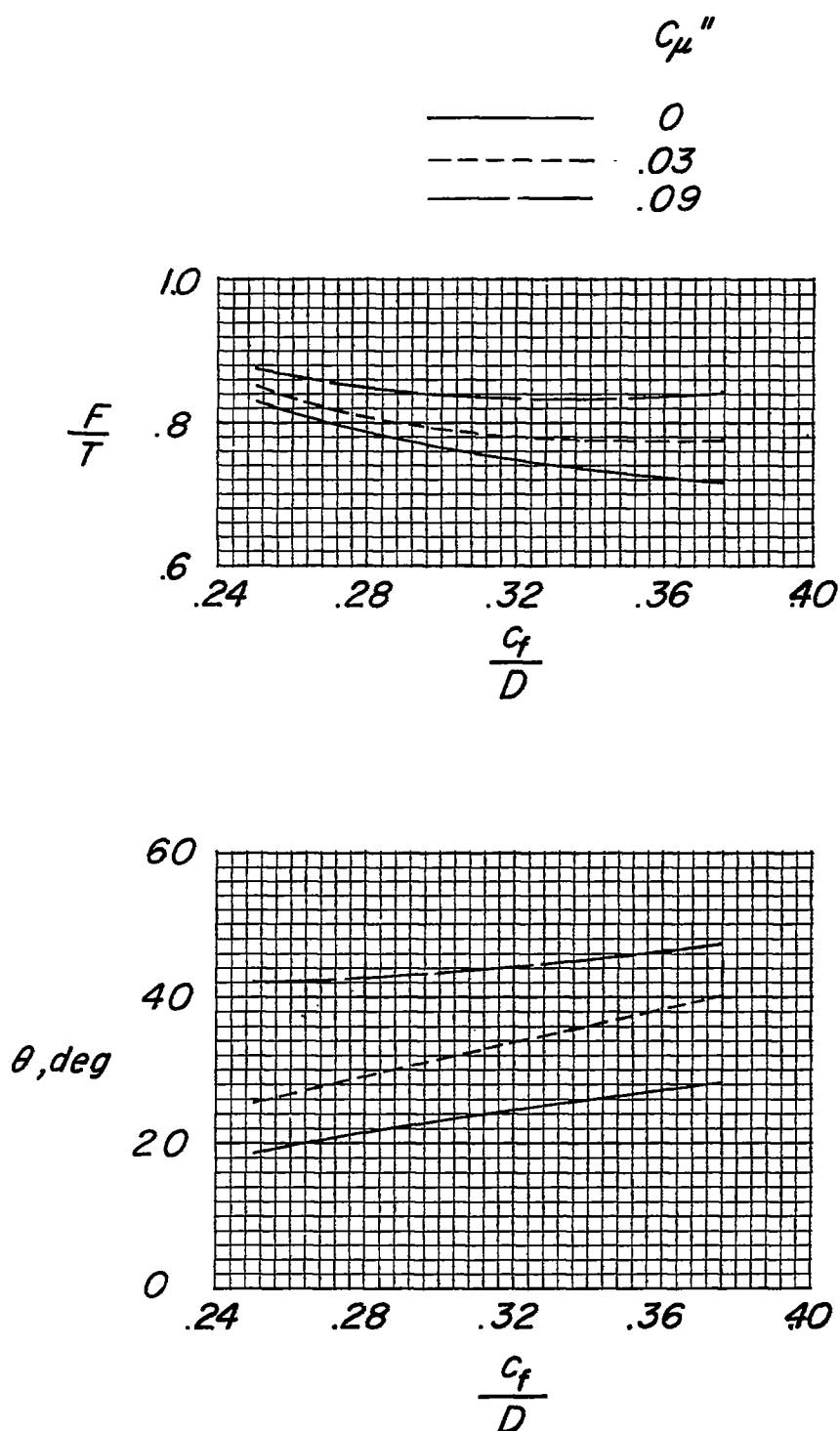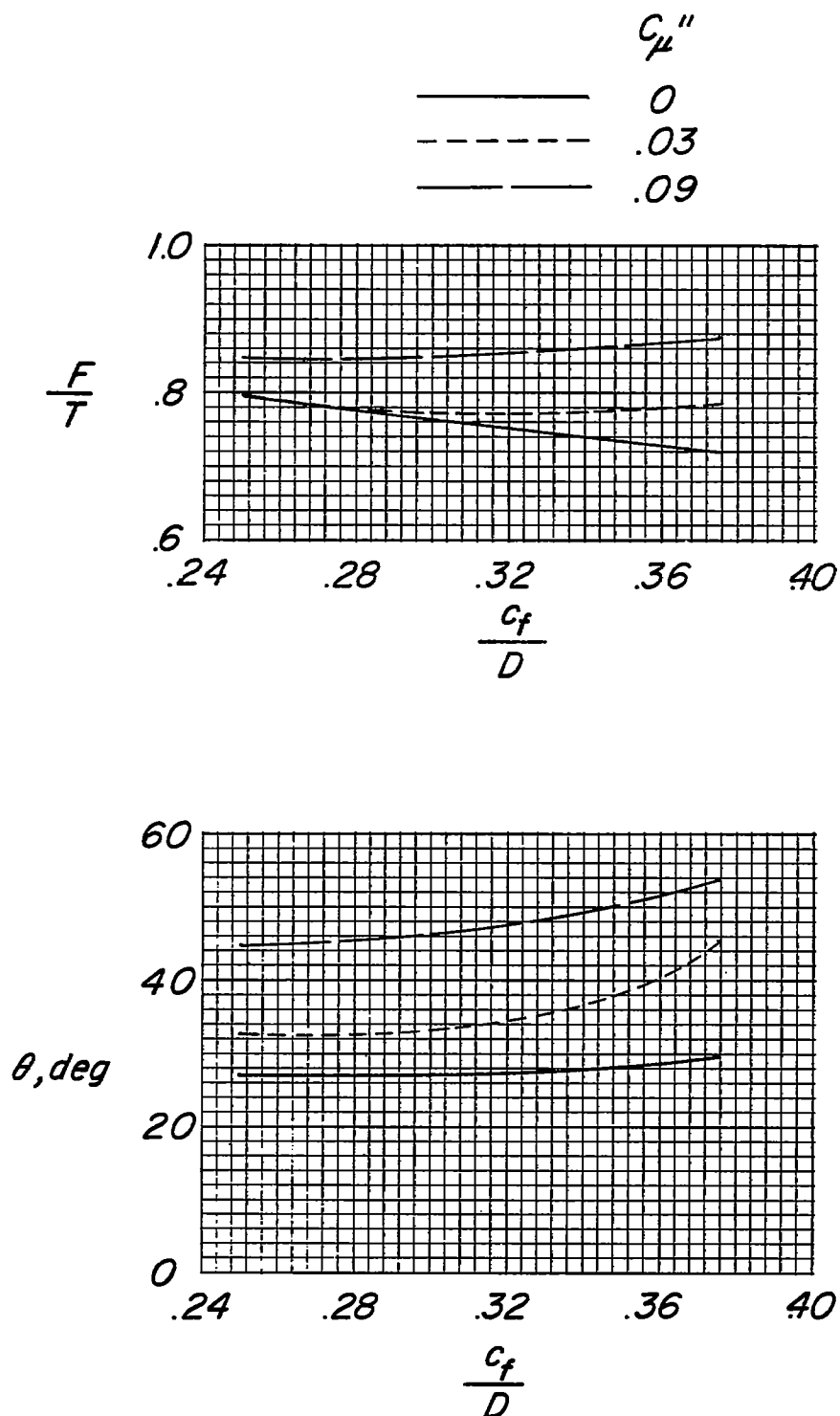
$$C_\mu''$$

————————— 0
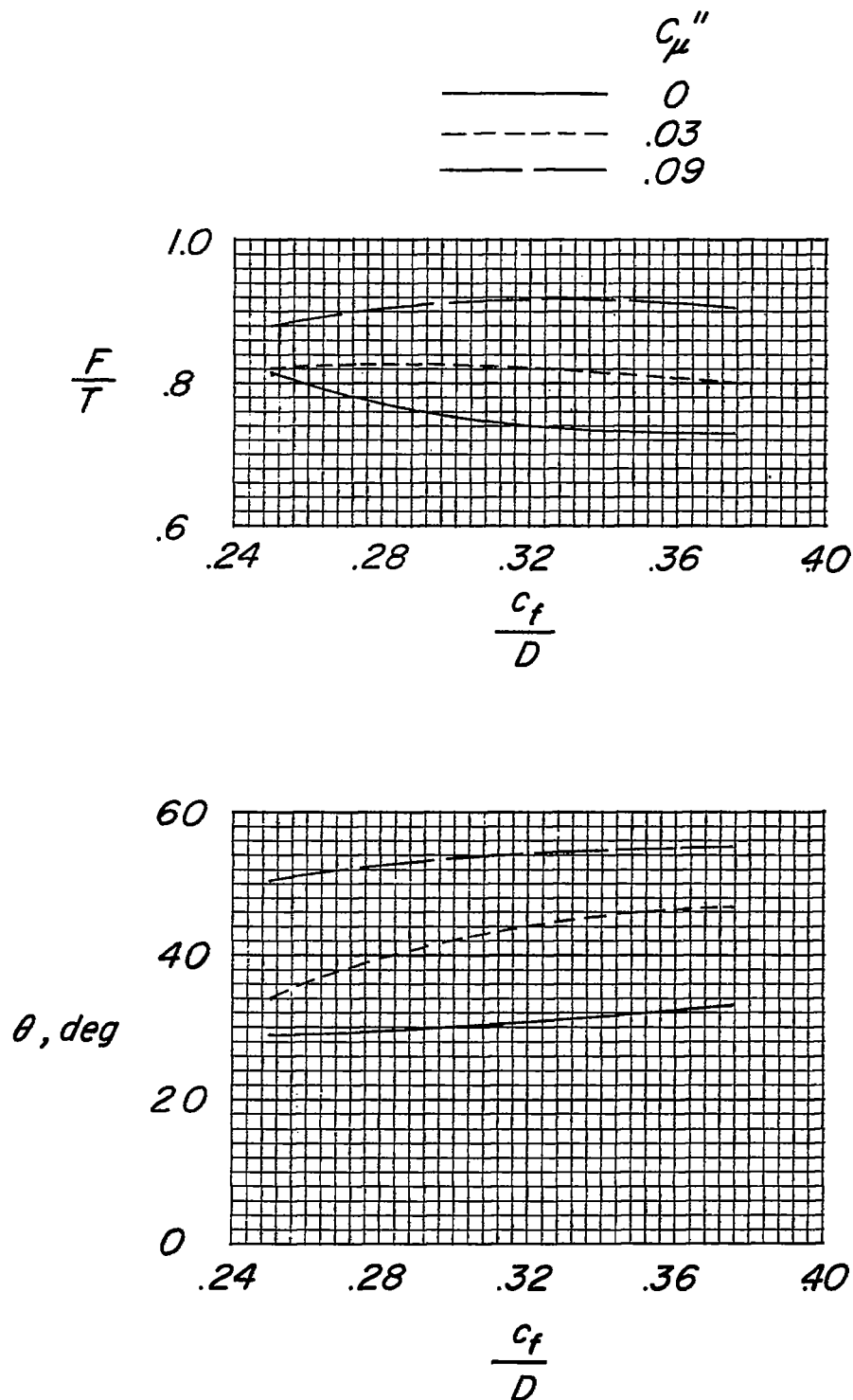
——————— $.03$

——— —— $.09$

Figure 21.- Effect of ratio of flap chord to propeller diameter on the ratio of resultant force to thrust and turning angle for a range of momentum coefficients. $\delta_{f,1} = 70°$; $\delta_{f,2} = 0°$; $h = 0.71$ foot.
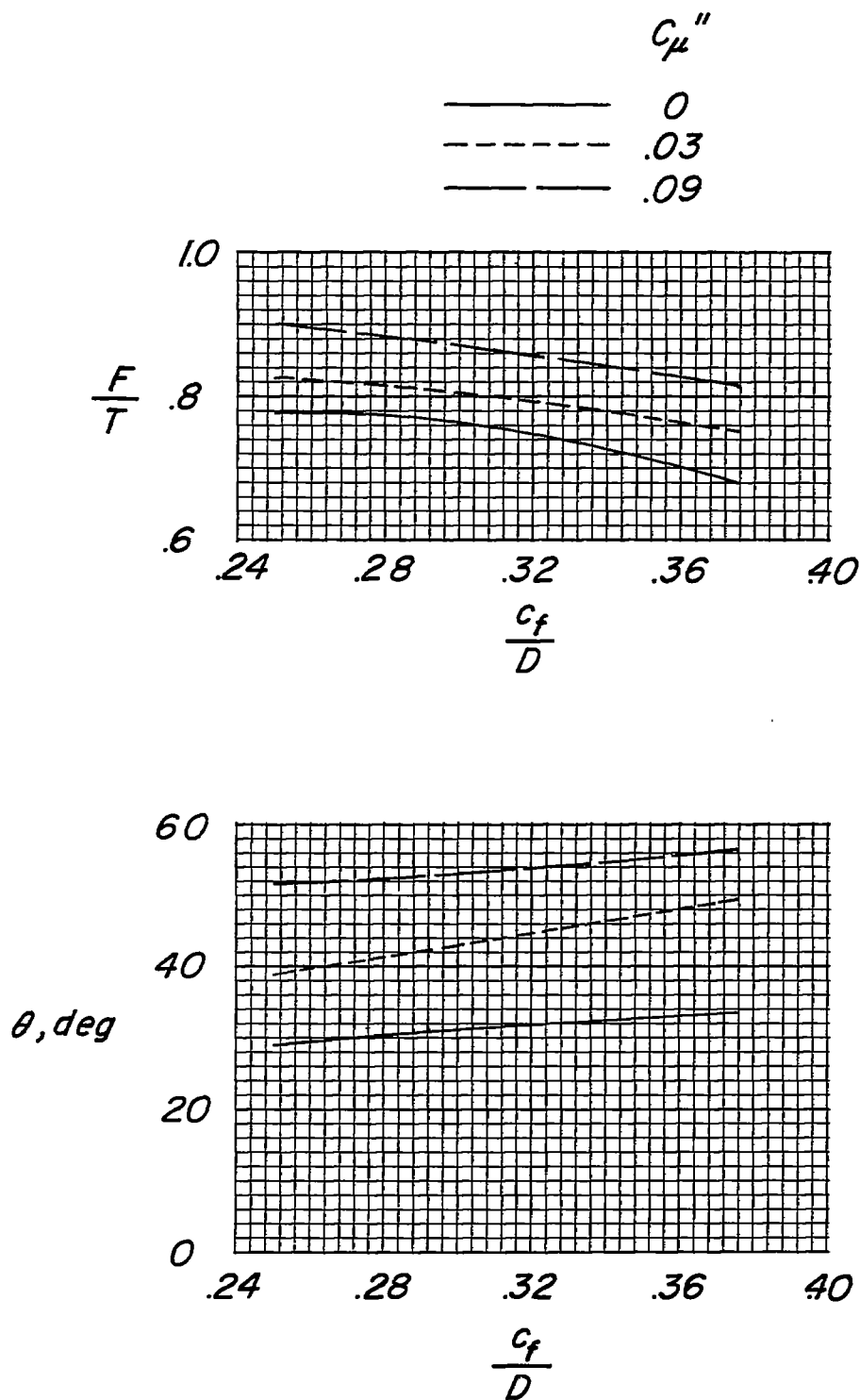
Figure 22.- Effect of ratio of flap chord to propeller diameter on the ratio of resultant force to thrust and turning angle for a range of momentum coefficients. $\delta_{f,1} = 70^\circ$; $\delta_{f,2} = 0^\circ$; h = 2.21 feet.
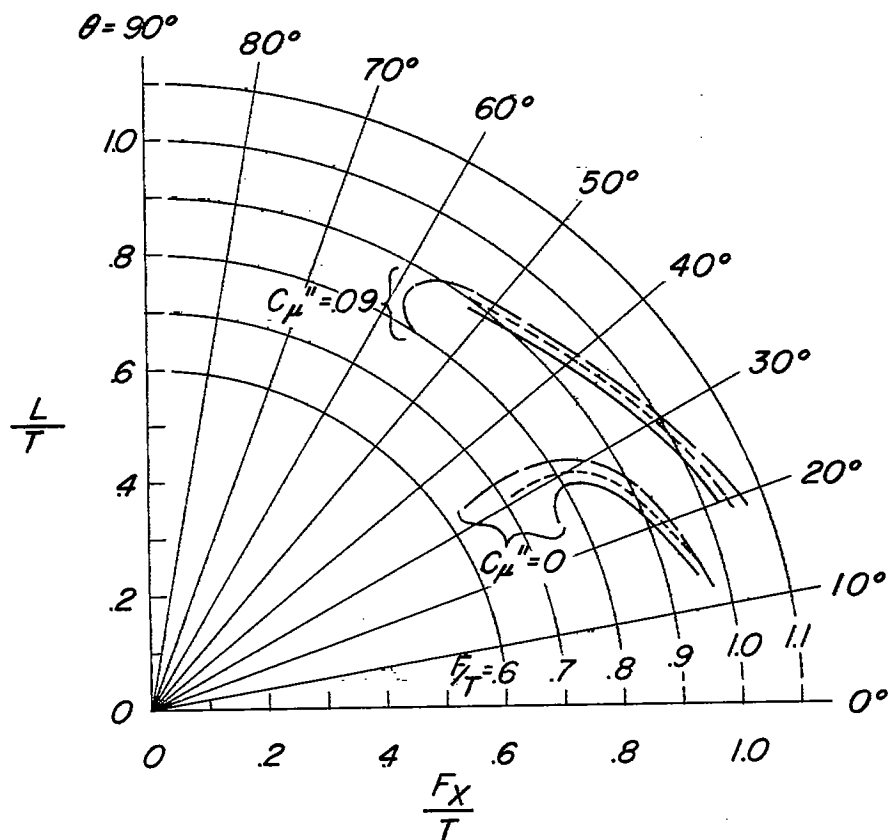
Figure 23.- Effect of ratio of flap chord to propeller diameter on the
ratio of resultant force to thrust and turning angle for a range of
momentum coefficients. $\delta_{f,1} = 70°$; $\delta_{f,2} = 0°$; $h/D \approx \infty$.

Figure 24.- Effect of ratio of flap chord to propeller diameter on the ratio of resultant force to thrust and turning angle for a range of momentum coefficients. $\delta_{f,1} = 60°$; $\delta_{f,2} = 30°$; $h/D \approx \infty$.

(a) Summary of turning effectiveness.
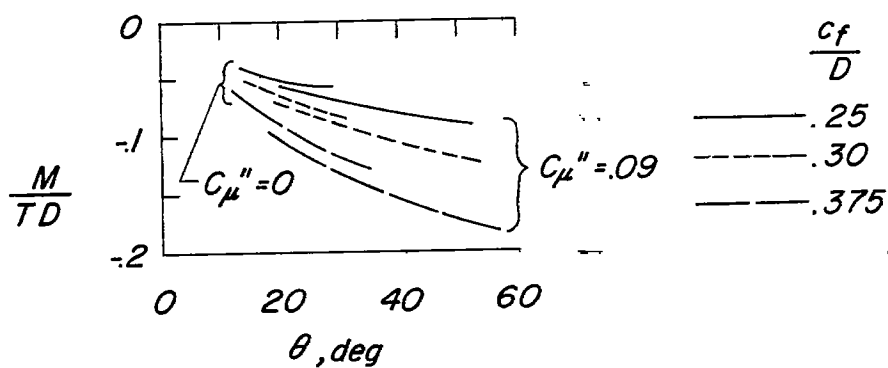
(b) Pitching moment.

Figure 25.- Optimum values at different flap deflections of ratio of resultant force to thrust, turning angle, and pitching moment. h/D ≈ ∞.
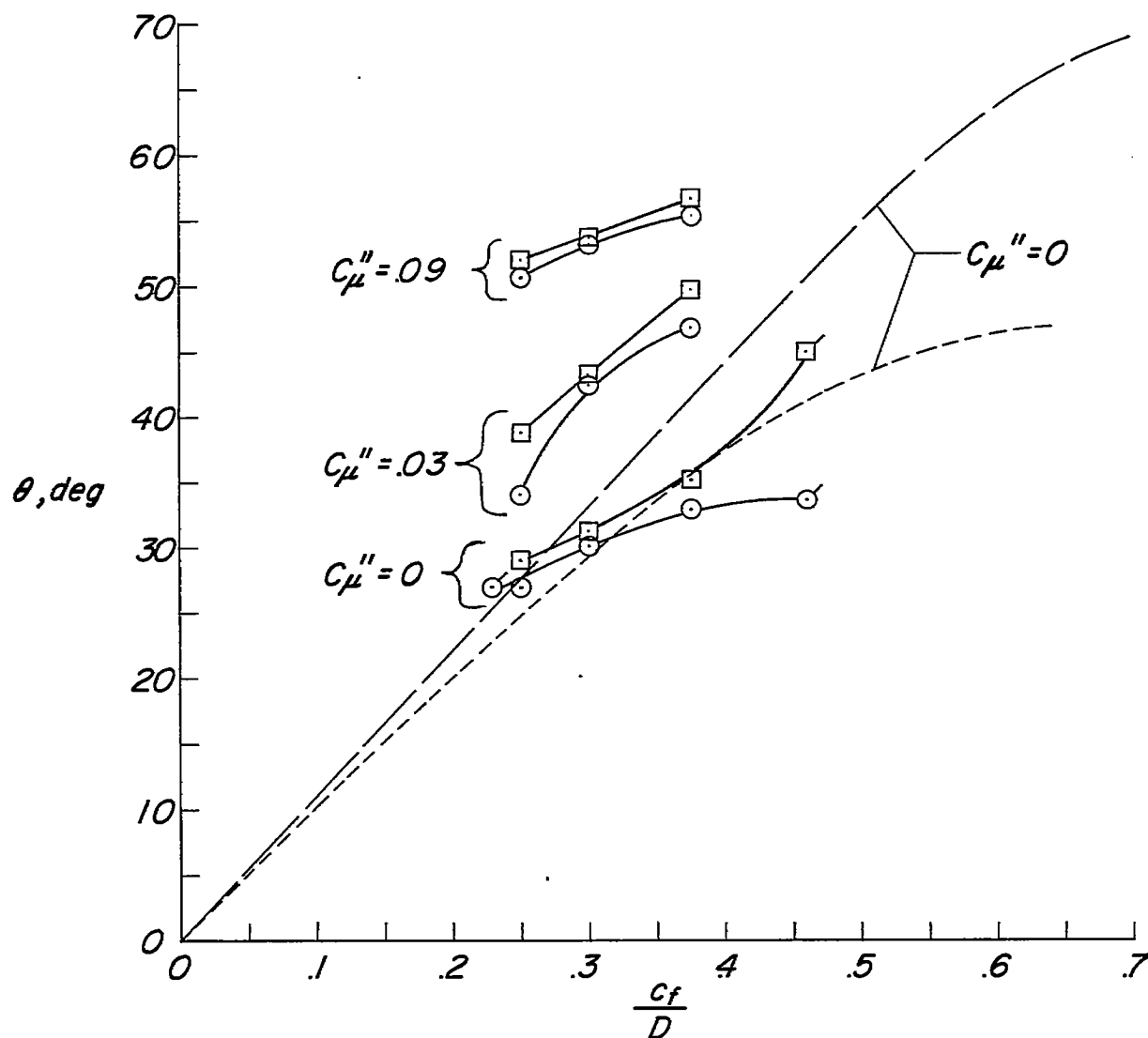
Figure 26.- Average variation of turning angle with ratio of flap chord to propeller diameter.